Report Prepared by :

S.C. Kranc and
Alberto. A. Sagüés

ADVANCED ANALYSIS OF CHLORIDE ION PENETRATION PROFILES IN MARINE SUBSTRUCTURE

Contract BB-880, USF # 2104 290 L0

Final Report to Florida Department of Transportation

Alberto A. Sagüés and S.C. Kranc
Principal Investigators
Department of Civil and Environmental Engineering

University of South Florida
Tampa, FL, 33620
January 31, 2003

1. Report No.	2. Government Accession No.	3. Recipient's Catalog No.
BB-880		

4. Title and Subtitle	5. Report Date
ADVANCED ANALYSIS OF CHLORIDE ION PENETRATION PROFILES IN MARINE SUBSTRUCTURE	January 31, 2003
	6. Performing Organization Code
	8. Performing Organization Report No.
7. Author's S.C. Kranc and Alberto. A. Sagüés	

9. Performing Organization Name and Address	10. Work Unit No. (TRAIS)
Department of Civil and Environmental Engineering University of South Florida Tampa, FL 33620	11. Contract or Grant No. BB-880
	13. Type of Report and Period Covered Final Report Sept. 1998 - Nov. 2002
12. Sponsoring Agency Name and Address Florida Department of Transportation 605 Suwannee Street Tallahassee, FL 32399-0450	14. Sponsoring Agency Code

15. Supplementary Notes
Prepared in cooperation with the U.S. Department of Transportation and the Federal Highway Administration

16. Abstract
The purpose of this investigation was to examine the suitability of more advanced transport models for chloride analysis, and of operator-independent procedures, to improve the accuracy of the analysis of chloride data from field extracted cores and related durability projections. The work conducted involved formulating the transport processes in concrete, examining alternative methods for sampling and analysis, and developing appropriate improved procedures. A user-friendly computer spreadsheet program was developed using those procedures. Alternative approaches to fitting slice data were developed, capitalizing on the observation that many profiles still maintain a “square root of time” dependence even if not reflecting simple diffusion. These techniques permit forward prediction of chloride intrusion, and with chloride binding information may provide much improved durability estimates. The effect of surface layers which produce “peaks” in the profile data was investigated also. Relatively simple modeling was found to provide a satisfactory estimate of the chloride profile. Modeling indicates that the carbonation/release mechanism had little or no effect on the total chloride profile ahead of the carbonation front, so that a square root of time dependence of the profile shape is maintained, facilitating durability projection. Core slicing strategies to optimize the prediction of chloride intrusion and minimize costs associated with analysis were developed. Chloride profile fitting procedures including time dependent diffusion and cylindrical geometries were examined. It was tentatively concluded that cores cut from typical cylindrical piles can be analyzed by assuming planar geometry. A new fitting procedure to include chloride binding was developed. If the potential for physico-chemical binding exists, the choice of a model for chloride intrusion will be impacted. It was concluded that in the presence of binding the simplified (Fickian) analysis will produce conservative (but not accurate) predictions of time to corrosion initiation. An advanced binding model was developed and tested, which produces binding parameter information from a total chloride profile alone.

17. Key Words	18. Distribution Statement
Reinforcing Steel, Corrosion, Chlorides, Concrete, Cores, Profiles, Durability, Forecast, Analysis	No restrictions. This document is available to the public through the National Technical Information Service, Springfield, VA 22161

19. Security Classif.(of this report)	20. Security Classif. (of this page)	21. No. of Pages	22. Price
Unclassified	Unclassified	87	

TABLE OF CONTENTS

EXECUTIVE SUMMARY... 3

OBJECTIVES AND OUTLINE 5

Section 1. INTRODUCTION 8

Section 2. TRANSPORT OF CHLORIDES IN SOUND, WATER SATURATED CONCRETE 10

Section 3. METHODS FOR ANALYSIS AND PREDICTION 17

Section 4. AN ADVANCED FITTING PROCEDURE INCLUDING THE EFFECTS OF BINDING AND CARBONATION 26

Section 5. STRATEGY FOR SELECTING SLICE DIMENSIONS AND ANALYSIS OF DATA 49

Section 6. CORROSION INITIATION TIME DERATING FACTORS FOR REBARS IN CONCRETE INCLUDING GEOMETRICAL EFFECTS 54

Section 7. OTHER COMPLICATING FACTORS 62

Section 8. SENSITIVITY STUDY 69

Section 9. REEXAMINATION OF PREVIOUS CORE SAMPLE DATA. 79

Section 10. PRINCIPAL CONCLUSIONS.. 83

BIBLIOGRAPHY 85

UNITS CONVERSION TABLE 87

NOTICE

The opinions, findings and conclusions expressed in this publication are those of the authors and not necessarily those of the State of Florida Department of Transportation. Prepared in cooperation with the State of Florida Department of Transportation. The assistance in the field investigations of personnel of the Corrosion group at the FDOT Materials Office is gratefully acknowledged.

EXECUTIVE SUMMARY

Corrosion of reinforcing steel in the substructure of Florida marine bridges is a major cause of deterioration requiring costly maintenance. The corrosion results from chloride ion penetration through the concrete. The FDOT has implemented numerous design guidelines and repair strategies to minimize this problem. Assessment of existing structures is routinely conducted to evaluate the success of the corrosion control methods, to forecast future corrosion performance, and to use the results to improve on current practice. A common form of assessment consists of extracting concrete cores and analyzing for chloride content as function of depth from the surface. A chloride concentration profile is thus obtained that can be analyzed to quantify the severity of chloride exposure and the permeability of the concrete. The present method of analysis is highly simplified, relying on assumption of simple (Fickian) diffusion for chloride transport and yielding an apparent diffusion coefficient (D) and an estimate of surface (C_S) and bulk (C_0) chloride concentrations in the concrete. Those parameters can be used in conjunction with an assumed value of critical chloride concentration to estimate how long it will take for active steel corrosion to start, a key value in predicting durability. However, this simplified approach is subject to many known limitations including inaccuracy from not accounting for complications in the transport processes (such as chloride binding), non-optimized sampling positions in the cores, and operator-dependent mathematical procedures for analysis of the data even under simplifying assumptions. The purpose of this investigation was to examine the suitability of more advanced transport models for chloride analysis, and of operator-independent procedures, to improve the accuracy of the analysis of field extracted cores and related durability projections.

The work conducted involved formulating the transport processes in concrete, examining alternative methods for sampling and analysis, and developing appropriate improved procedures. These activities produced several numerically sound approaches to determining the parameters C_S, C_0 and D for sliced specimens, requiring no operator intervention. A user-friendly computer spreadsheet program was developed using those procedures and prepared for delivery.

The results from several computational models to determine the variation in the profile for different assumptions were examined . Alternative approaches to fitting slice data were developed, capitalizing on the observation that many profiles still maintain a “square root of time” dependence even if not Fickian. These techniques permit forward prediction of chloride intrusion, and with chloride binding information may provide much improved durability estimates.

The effect of surface layers (for example from concrete carbonation) which produce “peaks” in the profile data was investigated also. Relatively simple modeling was found to provide a satisfactory estimate of the chloride profile. Modeling indicates that the carbonation/release mechanism had little or no effect on the total chloride profile ahead of the carbonation front, so that a square root of time dependence of the profile shape is maintained, facilitating durability projection. Core slicing strategies to optimize the

prediction of chloride intrusion and minimize costs associated with analysis were developed. Chloride profile fitting procedures including time dependent diffusion and cylindrical geometries were examined. It was tentatively concluded that cores cut from typical cylindrical piles can be analyzed by assuming planar geometry.

A new fitting procedure to include chloride binding was developed. If the potential for physico-chemical binding exists, the choice of a model for chloride intrusion will be impacted. It was concluded that in the presence of binding the simplified (Fickian) analysis will produce conservative (but not accurate) predictions of time to corrosion initiation. An advanced binding model was developed and tested, which produces binding parameter information from a total chloride profile alone.

OBJECTIVES AND OUTLINE

Objectives

Corrosion of reinforcing steel in the substructure of Florida marine bridges is a major cause of deterioration requiring costly maintenance. The corrosion results from chloride ion penetration through the concrete. The FDOT has implemented numerous design guidelines and repair strategies to minimize this problem. Assessment of existing structures is routinely conducted to evaluate the success of the corrosion control methods, to forecast future corrosion performance, and to use the results to improve on current practice. A common form of assessment consists of extracting concrete cores and analyzing for chloride content as function of depth from the surface. A chloride concentration profile is thus obtained that can be analyzed to quantify the severity of chloride exposure and the permeability of the concrete. The present method of analysis is highly simplified, relying on assumption of simple (Fickian) diffusion for chloride transport and yielding an apparent diffusion coefficient (D) and an estimate of surface (C_S) and bulk (C_0) chloride concentrations in the concrete. Those parameters can be used in conjunction with an assumed value of critical chloride concentration to estimate how long it will take for active steel corrosion to start, a key value in predicting durability. However, this simplified approach is subject to many known limitations including inaccuracy from not accounting for complications in the transport processes (such as chloride binding), non-optimized sampling positions in the cores, and operator-dependent mathematical procedures for analysis of the data even under simplifying assumptions.

It is desired to predict the time to chloride-induced depassivation of steel reinforcing in marine substructural elements with a high degree of confidence both for components already in service as well as those yet in the design phase. Excessively pessimistic or very conservative estimates are just as undesirable as overestimates, from an economic point of view.

In chemical analysis of field extracted cores total chloride concentration (rather than that of the free chloride in the pore water) is obtained. Grinding and mixing the powder from an individual slice produces a bulk averaged total concentration value over the extent of the slice, and located at the center. Thus, correlating the integrated data can be visualized as defining a “profile” of the chloride concentration, however the result is somewhat different than the actual distribution of chlorides.

Most physical evidence will be gathered early in the life of existing structures. For thick covers or long prediction times (from the time of measurement) the confidence attached to any projection will be obviously be reduced. Consequently, the goals of the present effort were to:

- obtain estimates of the Fickian parameters D, C_S and C_0 and examine how intrusion develops if alternative, advanced transport models are assumed.

- develop an efficient set of protocols and methods for the analysis of core data
- develop methods to predict the time to initiation of corrosion accurately and including confidence estimates if possible
- reexamine experimental measurements from earlier core samples

Ultimately, it may be possible to apply the results of this study to improve the computational damage function model, previously presented [1].

Outline of this report

Section 1 provides an introduction to the overall problem stated above. Numerous aspects of the problem and possible sources of error are considered.

Section 2 contains a brief discussion of diffusive transport in sound, saturated concrete, including the possibility of binding reactions. While diffusive transport is the primary mechanism of transport considered in this report, other mechanisms have been proposed and analyzed by others [2,3]. Later in this section, the analysis is extended to model the release of bound chlorides by progressive carbonation of the top layers of concrete. The binding mechanism seems most likely to be responsible for the observation of peaks and other distortions of profile data acquired from field-testing. One principal conclusion from this portion of the present effort is that relatively simple modeling of this mechanism provides a satisfactory estimate of the chloride profile and that furthermore the carbonation/release has little or no effect on the total chloride profile ahead of the carbonation front.

Section 3 outlines an elementary method for analysis of core slice data to recover a set of apparent values for D, Cs and C_0 assuming Fickian diffusion. The basis of this method is an optimization based on linear least square error regression. A simple Microsoft EXCEL spreadsheet version of an analysis program is provided (with instructions). Error analysis is discussed and prediction of time to initiation of corrosion is considered. Another subsection is concerned with prediction of time to initiation of corrosion, and accuracy of these predictions, especially when using several sets of modeling assumptions.

Section 4. This section contains a discussion of a more advanced technique (utilizing inverse methods) for model fitting, again based on optimization of minimal residual error but capable of handling models only expressed as differential equations. The advantages of this technique are numerous, more realistic models can be employed, in the case of binding accurate values for free chloride concentration can be obtained and as a side benefit, a chloride binding isotherm is generated.

Section 5 is devoted to the development of a slicing strategy based on the results of this investigation, intended to secure the maximum amount of information from cored specimens with a minimum of effort. Several issues regarding error are revisited.

Section 6 consists of an update and extension of the correction factor for the presence of rebars in estimating the time for initiation of propagation.

Section 7 is concerned with the influence of numerous complicating factors, including geometry, boundary conditions, and time dependent diffusion. The importance of cracks located in cored specimens were studied to some extent during this investigation but were reported elsewhere [4].

Section 8 reports the results of several sensitivity test procedures used to validate and further clarifies the work covered in previous sections. Some of these studies were conducted using synthetic core slice data obtained from earlier modeling efforts, other studies were completed by utilizing finely resolved and documented core data from the field.

Section 9 reports a summary of retesting of previously obtained and analyzed data

Section 10 summarizes the principal conclusions of this research and recommends future directions for similar efforts.

Section 1: INTRODUCTION

The transport of chlorides into sound concrete is often treated as a simple diffusional problem, but is in fact complicated by aging, binding, water transport, geometry, parameters variable in time and space, various external boundary conditions, cracks, and other factors, all of which are discussed more fully below. For lack of better techniques, inspection and prediction of the state of chloride ion penetration into concrete is usually accomplished by extracting and slicing transversely a cylindrical core sample, then analyzing the slice samples for concentration as a function of depth. This information is then fit to a Fickian model [5] to give predictions of lifetime, or alternatively a value for the diffusion coefficient that can be reasonably expected for various concretes. The choice of a Fickian model is due primarily to the lack of viable alternatives. Obviously, a number of assumptions are built into this process, most notably that the state of penetration of chloride ions is the result of a simple diffusional process. Furthermore, a tacit assumption that a slice sample can be homogenized and analyzed accurately for total chloride concentration. The transport process however, may in fact be quite complex and only approximate a diffusional process. The following questions need to be addressed:

a) How can the time to depassivation (or a diffusion coefficient) be accurately assessed from early profile measurements? Although the assumption of Fickian diffusion and a curve fitting procedure to best approximate the measured profile with an error function solution (see Section 3, equation 3.1) [5] may produce an “apparent” diffusion coefficient, this result may be conservative, and pessimistic estimates of lifetime may result in poor economic decisions.

b) While several groups have attempted to model complex transport processes, it is not clear how different these results are from those that would be predicted using “apparent” diffusion coefficients. If the assumption of a simple diffusional model to represent more complex processes is justified, this diffusion coefficient would be called an “effective” coefficient.

c) How physical sampling and analysis can best be accomplished, taking into account both accuracy in the determination of various parameters and economic considerations?

d) What techniques will result in the best forward prediction of service lifetime and what confidence can be attached to this estimate?

e) How sensitive are lifetime estimates to the following: (note that many of these factors contribute in a combined and possibly synergistic fashion)

> *Error*: Physical measurements are usually contaminated with error, both of an analytical chemistry nature (analysis of the chloride concentration) as well as error in the determination of physical position of the slice sample (e.g. due to the kerf of the saw blade or slant in the core cut). Furthermore, numerical

techniques utilized to approximate the data and smooth out scatter caused by measurement may suffer from limitations introduced by sample size and other factors.

Nature of the diffusion coefficient: Although systems are often modeled assuming a constant diffusion coefficient, in fact the diffusion coefficient may vary in time (due to aging of the concrete [6,7]), and space (possibly related to humidity transport and aggregate). Many of these cases have been treated in Crank [5].

Geometrical factors: While many problems are conveniently discussed in terms of one spatial variable, most structural elements have a multidimensional aspect. Examples include circular columns with azimuthal symmetry, corners, elements of finite thickness, and intersections of complex shapes. A related type of error is introduced by utilizing one-dimensional error function models to fit data taken from structural with three-dimensional characteristics (for example round columns).

Boundary conditions: The most common assumption regarding the boundary is to assume a constant surface concentration and a freely determined flux, but under many circumstances the concentration may be time dependent [8] or the flux limited (perhaps as some function of time, surface concentration or other external factors). Several authors have discussed a “skin” effect [9] and others have investigated surface microclimate effects [10]. On the surface of a structural element conditions may well vary with location [11].

In the following sections, consideration is given to the influence of each of these factors on the analysis of chloride penetration into reinforced concrete.

Section 2: TRANSPORT OF CHLORIDES IN SOUND, WATER SATURATED CONCRETE

The first subsection of this report briefly recaps diffusive transport and the development closely parallels similar discussions found elsewhere.

2a Diffusive transport in sound concrete including binding reactions

While it is recognized that a number of more advanced models have been suggested for chloride transport in sound concrete [2,3,12], in the present discussion, only a relatively simple model is necessary to address the questions posed in the introduction. To this end, a simple diffusional model to describe the transport of chloride through uncracked regions of concrete will be adopted, as described by others [12,13]. Transport is described in terms of an "effective" Fickian diffusion coefficient. Restricting transport of chloride ions through saturated concrete, for a liquid in the pores a one dimensional flux analogous to that in free water can be defined:

$$j_x = -D\frac{\partial C_f}{\partial x} \qquad 2.1$$

The diffusion coefficient D is understood to be similar to that of free water but modified by tortuosity and constriction (cf [14,15]). Here the lower case subscript f designates concentration in the volume of pore water rather than a material volume of porous concrete. To convert the concentration of free chlorides to a material basis (upper case subscript) requires division by the porosity since this ratio is equivalent to the open area/material area. Assuming porosity constant in space and time,

$$C_f = \frac{C_F}{\varepsilon} \qquad 2.2$$

The rate of change of total chlorides in a unit material volume per time is given by the flux of free chlorides, but transport is permitted only through the open pores. Then, based on the surface area of the material,

$$\frac{\partial C_T}{\partial t} = \nabla \cdot (\varepsilon j_x) \qquad 2.3$$

Thus the porosity factor is removed by cancellation and

$$\frac{\partial C_T}{\partial t} = \nabla \cdot (D \nabla C_F) \qquad 2.4$$

Many types of concrete show some evidence of chloride binding capacity and this mechanism is included here for generality. The total concentration of chlorides can be expressed in terms of the bound and free concentrations (material volume base) as

$$C_T = C_B + C_F \tag{2.5}$$

or, taking differentials

$$dC_T = dC_F\left(1 + \frac{\partial C_B}{\partial C_F}\right) \tag{2.6}$$

Substituting for the free chloride concentration, Equation 1 becomes (for the x direction)

$$j_x = \frac{-D}{1 + \frac{\partial C_B}{\partial C_F}} \frac{\partial C_T}{\partial x} \tag{2.7}$$

The time rate of change of total chloride concentration in a material volume is then equated to the flux of free chlorides into the volume, expressed in terms of the total concentration:

$$\frac{\partial C_T}{\partial t} = \nabla \cdot \left(\frac{D}{1 + \frac{\partial C_B}{\partial C_F}} \nabla C_T\right) \tag{2.8}$$

Boundary conditions are imposed at the concrete surface exposed to a saline solution. The pore water is assumed to be in equilibrium with the water at the surface in accord with Equation 2.2. At the other extreme, a semi-infinite condition can be imposed, or more conveniently for numerical work, an insulated condition deep in the concrete can be used to represent a plane of symmetry for a slab of finite thickness. At the sides of the computational region an insulated boundary condition is also imposed.

A simple model for binding [12,13,16-20] as a very rapid reaction has been adopted here, so that the bound and free chlorides are presumed to be in an equilibrium relationship which can be described by an idealized Langmuir isotherm (which is one of many possible relationships including simple linear binding[20]).

$$\frac{1}{C_B} = \frac{1}{C_F k C} + \frac{1}{C} \qquad 2.9$$

At small values of the free chloride concentration C_F, $C_B \approx k\, C\, C_F$, and the behavior approaches linear binding with a coefficient $k_o = k\, C$. At large values of C_B, $C_B \approx C$ and the behavior resembles unbound chloride diffusion since the binding effect has reached saturation. The diffusive transport in situations with no binding mechanism can be handled as a limiting case ($C_F = C_T$) and the result is the familiar Fick's law

$$\frac{\partial C_F}{\partial t} = \nabla \cdot (D \nabla C_F) \qquad 2.10$$

If the binding can be described by a linear mechanism, the same equation as 2.1 is obtained but with a reduced diffusion coefficient.

2b Profile peaks and the release of bound chlorides due to carbonation

While many profiles of total chloride concentration (obtained either from integrated models or actual experimental data) superficially resemble an error function distribution, discrepancies (i.e. bulges, peaks and other non monotonic behavior) have been observed and reported. A substantial number of profiles exhibit a peak near the surface (obviously, some consideration must be given to the sample dimensions and location). Since a profile having this characteristic gives the erroneous impression of a back flow of chlorides towards the surface and more importantly may affect conclusions about the rate at which chlorides build inside the concrete in time, it is of interest to examine some possible mechanisms for this behavior. Specifically, a complex interaction may exist between a small layer of carbonated concrete and a deeper region of uncarbonated concrete in which the chlorides are bound by physico-chemical mechanisms. It has been further suggested that as the carbonation front moves into the concrete, bound chlorides are released [21]. Changes in diffusion coefficient and porosity might also occur (while the present discussion focuses on carbonation, similar situations include sulfate interaction, biofouling etc as well as applied barrier layers).

The goal of the present discussion is to examine the underlying causes of particular profile characteristics observed during physical sampling. While some apparent features may be due simply to error, it is also true that these characteristics may be due to mechanisms other than simple diffusive transport, and so may have important implications when attempting to fit to error function profiles. Transport at least partially due to physicochemical binding of the chloride ions is of particular interest. To help resolve these issues, the following cases are of interest and have been modeled.

a) Initially sound, uncarbonated concrete, exposed to combined CO_2 and Cl^- ion attack. The cement paste supports some reversible chloride binding. The chlorides penetrate faster than the carbonation front is moving. Release of bound chlorides occurs at the front. Changes in porosity and diffusion coefficient are neglected in the present discussion but could be considered. Modeling assumptions include both a simple linear variation across a relatively thin layer of carbonated concrete Since the front is moving across a stationary grid, computations must accommodate the conditions at the interface

b) Same assumptions as (a) except that for the linear gradient in the carbonated region, a more advanced treatment assuming Fickian diffusion across this layer is imposed.

c) Initially sound concrete capable of binding has developed a carbonated layer of some finite thickness prior to exposure to a chloride laden environment. For simplicity the carbonation front is assumed to be stationary. A complete solution for the diffusion equations on both sides of the interface has been obtained. The interface is treated by applying jump conditions to the governing differential equation.

To model the moving front, the following assumptions are imposed:

1. The concrete is divided into two regions, Region1, representing the carbonated layer extends from the surface to the sharp boundary (denoted i) where carbonation ends. Region 2 extends from this point to infinity.

2. In both regions, the porosity and diffusion coefficient are constant but may be different. Everywhere the concrete is fully saturated with water. These assumptions are made for simplicity and could be relaxed.

3. The carbonation front moves at a rate [22] such that the thickness is given by

$$X_i = R\, t^{1/2} \qquad 2.11$$

where R is the constant of proportionality and the velocity is

$$V_i = \frac{R}{2\sqrt{t}} \qquad 2.12$$

4. Binding in Region 2 is governed by an equilibrium Langmuir isotherm:

$$\frac{1}{C_B} = \frac{1}{\varepsilon C_F k C_C} + \frac{1}{C_C} \qquad 2.13$$

5. Since there is no binding in Region 1, the surface concentration related to the surrounding environmental concentration by

$$C_{T1} = C_{env}\,\varepsilon_1 \qquad 2.14$$

6. The carbonated layer is sufficiently thin that the flux may be represented by

$$\frac{\partial C_T}{\partial x} = D_1 \frac{C_{T0} - C_{1i}}{X_i} \qquad 2.15$$

Alternatively, a full diffusional model in this region may be imposed.

7. At the boundary the pore water must contain the same amount of free chlorides on both sides

$$C_{f1} = C_{f2} \qquad 2.16$$

(the lower case f denotes free concentration in the pore water)

8. There must be no accumulation of chlorides at the boundary. For a moving boundary this condition is represented by combining the diffusive and convective transport across the boundary [5] according to

$$\left[D_1 \frac{\partial C_{T1}}{\partial x} + \frac{D_2}{1+C_B'} \frac{\partial C_{T2}}{\partial x} - V_i C_{T1} + V_i C_{T2}\right]_i = 0 \qquad 2.17$$

where

$$C_B' = \frac{\partial C_B}{\partial C_F} \qquad 2.18$$

9. At infinity, the concentration must equal the background concentration.

10. In Region b the concentration is governed by Fick's second law subject to the equilibrium binding isotherm (assumption 4 above)

$$\frac{\partial C_T}{\partial t} = \frac{\partial}{\partial x}\left(\frac{D}{1+C_B'}\right)\frac{\partial C_T}{\partial x} \qquad 2.19$$

A substantially different computational approach is required than for simple diffusional models. To solve the governing equations, a central space-forward time finite difference scheme has been implemented. At every time step, the position and velocity of the carbonation front must be recomputed and to satisfy the flux condition it is necessary to solve for the concentration of free chloride in Region a at the boundary in terms of that on the opposite side. The total chloride concentration in Region b at the boundary can then be deduced so that the computations can proceed to the next time step. Auxiliary equations must be solved to account for the position of the front between nodes in the numerical grid. When solving the full diffusional model for the released region, a starting solution for small time is required.

To model the case of a pre-carbonated layer that is not growing (stationary front), the same assumptions listed above are employed, except that the distribution of concentration in Region a is computed from Fick's second law rather than imposing a simple linear gradient. Because no variable grid spacing is required, the computation can proceed directly.

As an example problem, the following conditions are specified. R is chosen so that the carbonation front is at 0.32 cm at three years age. D=4e-9 cm^2/s, C_S=25 kg/m^3, and C_0=0.15 kg/m^3.

Results at 3 years and 30 years are depicted in the figure below. Results for a similar binding situation with no release are shown for comparison. The case of a stationary, precarbonated layer yields similar results to the moving front models except that the concentration of chloride ions shows a slight increase at the interface. Finally, it is noted that the distribution of concentration across the precarbonated layer is very linear except for very early in the exposure period, which tends to support the linearity assumption made in the previous case.

As discussed elsewhere, modeled results can easily be analyzed as hypothetical data (by computing integrated “slices”) and subjected to various tests involving sampling and prediction. A moving carbonation front produces the expected profile. When subjected to data analysis techniques, the slicing process produces the characteristic peak. Clearly, the flux is not reversed but does appear to be. If the differences in porosity and diffusion are not large, the profile closely approximates the binding profile that would have been obtained without carbonation.

Finally, it should be noted that the above treatment assumed similar chloride diffusivity for the carbonated and uncarbonated regions. The analysis could be easily updated to include differences in diffusivity between those regions.

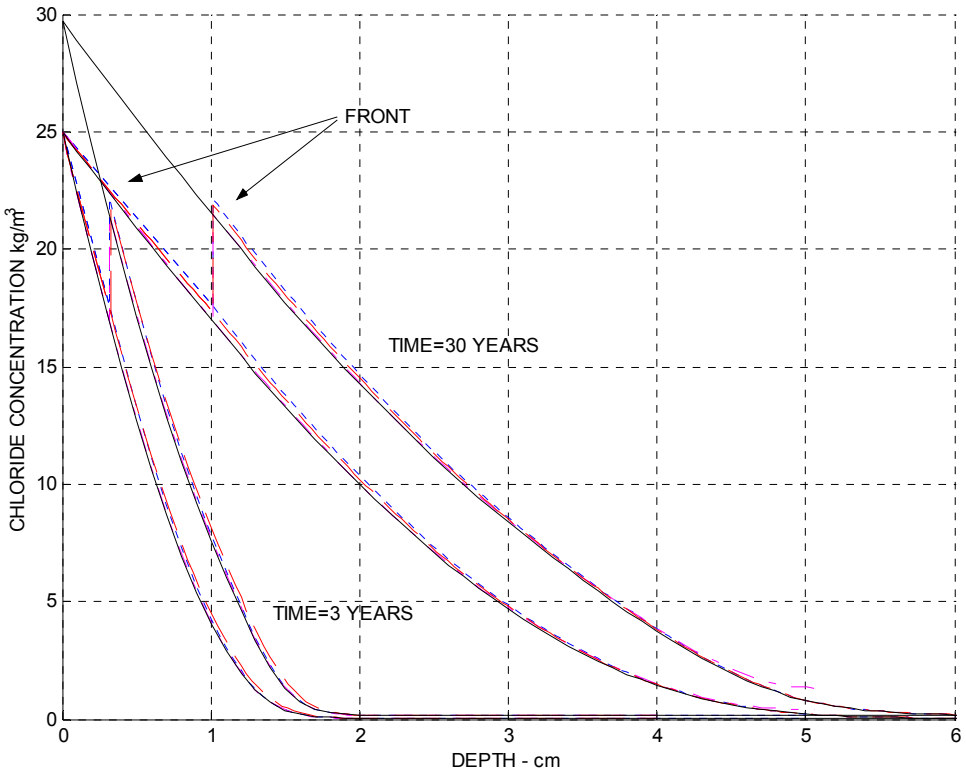

Figure 2.1. Total and free concentration for example discussed above at times 3 years and 30 years. (solid, no release; -- full diffusional model with moving front; …. linear gradient model; -.-. stationary front)

The fundamental conclusions of this portion of the study are that

a) All three computational models for release produce very similar results for the case investigated. The assumption of a linear profile for the free chloride profile in the released region is quite satisfactory and there appears to be little reason to compute a full diffusional model for this region.

b) The results produced by the computational models are only slightly greater than assuming a front position, then postulating a free chloride profile with no binding up to this point followed by a total chloride profile including binding.

c) If required any of these models could be used to generate ideal data to produce synthetic slice data for trial analysis. The results exhibited here tend to support the protocol of evaluating the first slice carefully and either discarding it or using this information to model the carbonated layer. It is noted that an estimate of the rate of carbonation could be obtained from this step.

Section 3. METHODS FOR ANALYSIS AND PREDICTION

The material discussed in Sections 3, 4, and 8 is concerned with fitting experimental data to proposed models of various degrees of complexity. It is advisable to remember that this process validates no model, and the only result is parameter estimation for the particular model investigated. Although frequently utilized as a goodness of fit test, improvements in residual error do not necessarily indicate a better physical model.

3a Elementary analysis based on error function solution

One of the simplest model for transport of chloride ions in porous media is given by Fickian diffusion (Equation 2.1). In this treatment, a diffusion coefficient constant in time and space is assumed. For one dimensional conditions, assuming an undisturbed condition at infinity, the well known complimentary error function solution results

$$\frac{C - C_0}{C_S - C_0} = \operatorname{erfc}\left(\frac{x}{\sqrt{4Dt}}\right) \qquad 3.1$$

As mentioned above, to determine the extent of chloride penetration into concrete a common practice is take a core sample, then slice and analyze the sample, producing a representation of concentration as a function of depth. Various transport mechanisms for the penetration of chloride ions into concrete can be calculated in highly resolved detail by computational modeling. By integrating these results over the dimensions of proposed slices, an idealized data set can be obtained, suitable for the same methods of analysis used for actual data. The advantage of this approach is that it is also possible to see exactly what will happen in the future, so that any data analysis technique can be simulated and evaluated.

The basis of this method is to fit slice integrated spatial distribution data for chloride ion concentration to the well known complementary error function as given above. It is possible to solve for the parameters by an exhaustive search method, but a method based on least square error residuals has been selected here. An alternative, equivalent representation to Equation 3.1 is

$$C = C_S \operatorname{erfc}\left(\frac{x}{\sqrt{4Dt}}\right) + C_0 \operatorname{erf}\left(\frac{x}{\sqrt{4Dt}}\right) \qquad 3.2$$

The data are assumed to be slices of variable thickness located at arbitrary depths into the concrete. Total chloride concentration is sampled. The depth of the sample is assumed to be the midpoint of the slice. While for thin slices the midpoint value of the

error function could be assumed, this approximation can be poor, especially if the slice is thick. Thus the i^{th} data point can be approximated by

$$C = C_S \frac{1}{\delta l_i} \int_{\delta l_i} \text{erfc}\left(\frac{x}{\sqrt{4Dt}}\right)dx + C_0 \frac{1}{\delta l_i} \int_{\delta l_i} \text{erf}\left(\frac{x}{\sqrt{4Dt}}\right)dx \qquad 3.3$$

where δl_i is the thickness of sclice i.

For any given value of D this is a linear model in C_S and C_0, as discussed previously. Least square linear regression methods can be applied to a set of n points. The quantity to be minimized is (as usual) the square of the difference between the model and the function yielding the optimum values for C_S and C_0 for a particular value of D.

$$e^2 = \sum_{i=1}^{n} [C_S \phi_{1i} + C_0 \phi_{2i} - C_i]^2 \qquad 3.4$$

where

$$\phi_{1i} = \frac{1}{\delta l_i} \int_{\delta l_i} \text{erfc}\left(\frac{x}{\sqrt{4Dt}}\right)dx \qquad 3.5$$

and

$$\phi_{2i} = \frac{1}{\delta l_i} \int_{\delta l_i} \text{erf}\left(\frac{x}{\sqrt{4Dt}}\right)dx \qquad 3.6$$

These functionals represent means of the error function and the complement at the mid point depth of slice and usually have similar magnitudes. Attention is called to the identity (for computation)

$$\phi_{1i} = 1 - \phi_{2i} \qquad 3.7$$

For any value of D, linear regression can be used to compute a value for C_S and C_0, then Equation 4 can be optimized for the value of D producing the minimum residual

error, noting that the values of the linear functionals change as D changes. Pearson's R is an alternative test of goodness of fit. Taking a broader view of the fitting process, because the error function solution is self-similar, it is the product Dt_m that is actually generated by the fitting process, so that errors in t_m are reflected inversely in the value of D obtained. The same method can be applied in situations where C_0 is known, eliminating one variable, as discussed below

The advantage of this alternative formulation is that the problem of fitting the data is reduced to a sequence of subproblems: the problem of finding the best C_S and C_0 for a particular D. The model consists of the linear superposition of two basis functions that are not similar in appearance. Standard linear regression techniques are easily applied to this problem and no previous knowledge of C_S and C_0 is required. For any combination of C_S and C_0 the sum of residuals (in the least square error sense) can be computed, then minimized by using a non-linear optimization algorithm or search (both are available in spreadsheet toolboxes). The problem of determining the best C_S, C_0 and D in situations where some constraints on these parameters are available is somewhat different and should be considered further.

Once all three free parameters have been obtained, it is tacitly assumed that the results can be extended to the original model equation to produce a continuous distribution. It should be noted that this assumption is significant and will be discussed in more detail later. A prediction of time to initiation for threshold concentration C_{crit} at cover depth X_c can be obtained from

$$\mathrm{erf}^{-1}\left(1-\frac{C_{crit}-C_0}{C_S-C_0}\right) = \frac{x_c}{\sqrt{4Dt_i}} \qquad 3.8$$

A remaining problem is to ensure that no other solution for C_S, C_0 and D is nearly as good as that with a minimum residual. Two widely different sets of fitted parameters could give nearly the same residual error and furthermore that the fitted set may not accurately represent the position of the moving front of critical concentration at the time of observation. If a widely divergent solution exists and lies close to the optimal by the criterion of residual error then the choice of a "correct" solution may be ambiguous. The location of a final solution would have to be checked, as well as other solutions which are nearly as good as the best.

A variation of this method is to utilize a deep slice to estimate C_0, which reduces the degrees of freedom to 2. For any value of D, C_S can be directly calculated by differentiating the error expression in Equation 4 with respect to C_S and setting equal to zero.

$$C_S = \frac{\sum_i C_i \phi_{1i} - C_0 \sum_i \phi_{1i}\phi_{2i}}{\sum_i \phi_{1i}^2} \qquad 3.9$$

for any value of D as before, except that C_0 is inserted as data. Then the value of D minimizing the error set can be optimized.

Using this expression it is easy to calculate the sensitivity of C_S to C_0

$$\frac{\partial C_S}{\partial C_0} = \frac{\sum_i N_{1i}N_{2i}}{\sum_i N_{1i}^2} \qquad 3.10$$

Thus the dependence of C_S on C_0, does not depend on the concentration data directly but only through the product Dt_m and the slice geometry. Similar reasoning shows that the dependence of C_S on any particular data point C_i is determined by $\phi_{1i,}$ and since the value of ϕ_{1i} decreases with depth, data near the surface are most important, for some particular value of D.

3b Time to corrosion initiation

Ultimately, one important goal of the coring, slicing and analysis procedure is to produce an estimate of the time to initiation of active corrosion. In the case of Fickian diffusion, the motion of the critical concentration depends on the square root of time (it can also be shown that profiles including binding have this property). For example, the Fickian solution at the time of sampling, t_m, is given by

$$\frac{C_m - C_0}{C_S - C_0} = \mathrm{erfc}\left(\frac{x_m}{\sqrt{4Dt}}\right) \qquad 3.11$$

where C_{cr} is the critical concentration for depassivation. Taking advantage of the self-similar character of the solution, a comparable expression can be written for the time of initiation, t_i, at some cover depth x_c

$$\frac{C_{Cr} - C_0}{C_S - C_0} = \mathrm{erfc}\left(\frac{x_C}{\sqrt{4Dt_i}}\right) \qquad 3.12$$

Combining these two equations and taking the inverse error function on both sides yields the simple relationship

$$t_i = t_m \frac{x_c^2}{x_m^2} \qquad 3.13$$

Any model for chloride intrusion having a square root of time dependence (or nearly so) could be analyzed in this fashion.

To obtain x_m, the current location of critical concentration at the time of measurement, either an analytical solution (such as the complementary error function) or an interpolation procedure is required. Thus if at some time t_m the profile is measured and the position x_m of the critical concentration is calculated, the time to depassivation t_m at the cover depth x_c can be immediately determined. If the model is a simple Fickian curve the answer will be the same (within error limits) as that obtained from the fitted C_S, C_0 and D by computing the inverse error function. Determination of the time of initiation then is dependent on accurate measurements of x_m. It is possible to use variations of the first method as described above to do the interpolation procedure, but it is also possible to directly fit the slice data.

The underlying premise is that the location of the point of critical concentration is determined (or approximately determined) for all time by a square root relationship. Thus for simple diffusion all the information available through the parameters C_S, C_0 and D, is equally available by determining this position at the time of observation. Utilizing methods providing the highest degree of accuracy (as well as knowledge of the time) is essential since inaccurate measurement of x_m will produce a poor estimate of t_i.

It is important to emphasize that forward predictions can be made only by assuming the motion of the profile in time. It is not necessary to identify an underlying model for the transport process, only to be confident of this assumption. While the error function (or other similar solutions) may be utilized, it is also possible to utilize a simple polynomial model due to the small number of data points. The background and the critical concentrations are close in value, a fact that must be considered in the interpolation scheme. Finally, the assumption that for each slice the mean value may be located near the center of the slice my be sufficiently accurate that the data can be fit directly without regard to integrating the underlying profile.

It is worth noting that the number of data points (slices) is quite small for this type of fitting procedure. As more parameters are included this problem becomes worse. While the material here has focused on traditional least square analysis, general optimization methods can easily be utilized to accomplish the same result. This discussion will be extended to binding models in the next section.

3c Error in forward prediction of time to initiation

Equation 3.13 above can be used to assess the relative error in t_i assuming x_c, x_m, t_m are all contaminated by error. Thus the relative error is given by

$$e = (1 \pm 2\frac{\Delta x_c}{x_c})(1 \pm \frac{\Delta t_m}{t_m})(1 \pm 2\frac{\Delta x_m}{x_m}) \qquad 3.14$$

where

Δx_c= absolute error in rebar cover dimension

Δx_m= absolute interpolation error for critical front at time of observation

Δt_m= absolute error in time to observation

Note that Δt_m could be as much as two years (because of limited record keeping). The goodness of fit criterion is difficult to apply to the interpolation of the position of the critical front, for the same reason that it is not possible to compare the slice data to the analytical prediction of an error function made. The error in the estimated depth of penetration of the critical concentration at the time of observation Δx_m is the combination of several error sources as discussed previously, and may be measured directly or computed using a function model.

The results of numerical calculation of the position of the critical concentration indicate that a similar relationship dependent of the square root of time is obeyed very closely for a number of models which are not simple error function profiles. Estimating C_S, C_0 and D to predict the time of depassivation will not produce the same result as the direct calculation based on current position unless the fitted profile model at the time of observation agrees closely with the actual position of the critical concentration. For many models this is not the case. Furthermore if the fitting procedure yields a poor value of the surface concentration, the predictive results will also be poor. Regarding Method 2, if applied in situations where the motion of the threshold concentration is not really root time dependent, then obviously the prediction will be in error.

Many fitting procedures generally available produce results with distributed error over the interval. It may be desirable to utilize techniques emphasizing goodness of fit near the point of interest. Certainly data with near surface peaks suffer from poor results elsewhere and a fitting procedure which skips the first data point can be used to partially offset this problem. One other possibility is to use weighting techniques for the residual error. While an intriguing possibility, considerable analysis would be necessary to

implement this idea. It would also be possible to concentrate the data slices near the point of interest. Yet another approach based on a partitioned model has been developed. The discussion of this method is deferred until a later section.

3d Error in evaluation of other parameters

Error in the evaluation of underlying parameters C_S, C_0, and D can be estimated in the following manner. In this analysis for simplicity the error function is used as a typical fitting shape. It is assumed that similar values for error estimates would be obtained for other models.

Starting from the general expression for fit error but adding a term to account for measurement error in C_i

$$e^2 = \sum_{i=1}^{n} [C_S \phi_{1i} + C_0 \phi_{2i} - C_i \pm \Delta C_i]^2 \qquad 3.15$$

The error term ΔC_i may be known in absolute or relative terms from independent estimates, or may be estimated from the scatter associated with a fitting procedure. Assuming for the moment that D is known exactly and C_0 is known accurately from background measurements, the value for surface concentration will be computed as

$$C_S \pm \Delta C_S = \frac{\sum_i C_i \phi_{1i} - C_0 \sum_i \phi_{1i} \phi_{2i} \pm \sum_i \Delta C_i \phi_{1i}}{\sum_i \phi_{1i}^2} \qquad 3.16$$

This value will include the uncertainty introduced by experimental measurement error so that an approximate maximum bound on the error associated with C_S is

$$\Delta C_S = \pm \frac{\sum_i \Delta C_i \phi_{1i}}{\sum_i \phi_{1i}^2} \qquad 3.17$$

This value lacks the normal statistical considerations associated with least square methods but is probably satisfactory given the small number of data points involved. Errors in the fit for D are ignored at this point. Again, the value of ΔC_i may be proportional to C_i or may be an absolute quantity, depending on the nature of the experimental error.

To estimate the error in the determination of D, assuming that the surface and background concentration are known exactly is the same as minimizing e^2 by variation of D (affecting the basis functions only). Thus the solution to

$$\frac{\partial}{\partial D}\sum_{i=1}^{n}[C_S\phi_{1i} + C_0\phi_{2i} - C_i \pm \Delta C_i]^2 = 0 \qquad 3.18$$

is needed and a numerical evaluation will be required, after appropriate terms for ΔC_i have been inserted.

3e The FITTER program

A spreadsheet program to analyze both actual measurements as well as computational results has been developed. Program FITTER relies on the SOLVER function and the erf function in Microsoft EXCEL, both of which must be installed for the program to operate. This program has been conveyed to FDOT separately from this report.

1. This program (FITTER) is a conventional EXCEL program with macros. The program media has been swept for viruses in a relatively up-to-date checker. The macros need to be active to run the program.

2. Up to twelve data points can be entered (the maximum depth is 23 cm but this is arbitrary). The format is "midpoint - thickness", thickness interpreted as full slice dimension rather than half thickness (could also be "start-finish" with modification). The data entry form requires blank or zeros after the last point. The program will not accept a zero data point with a positive data point deeper. Data can be entered in centimeters or inches, but this choice must be selected with the button toggle. Concentration units are arbitrary but must be consistent. To indicate units correctly in the results, use the toggle.

3. Two methods are implemented. One makes an estimate of Co while the other uses input. If the background concentration is known it should be entered, else enter zero (or an estimate). Cs, Co and D are first obtained, then Cs and D are obtained based on knowledge of Co.

4. The actual fitting process (click on "FIT") can be lengthy, several minutes possibly depending on computer speed. A warning "ACTIVE" will be replace by "DONE". Occasionally the SOLVER dialog may report that the maximum time is exhausted. Just click on STOP or possibly KEEP SOLUTION. It is possible that one or both methods may fail, and this is so indicated.

5. The graph shown on the spreadsheet depicts the original slice data and both fit profiles generated from the erf-erfc underlying model. Because the data is slice averaged, the fit may not appear to be particularly good. It will probably be necessary to rescale the graph, since this is not handled automatically. All zero data points are clustered at the given value of Co and at a depth of 23 cm.

Program warnings and cautions:

1. This program was prepared for FDOT use and not intended for open or commercial distribution.

2. This program is considered to be in development. As such, no guarantees are made concerning accuracy or suitability for design or economic decisions.

3. As indicated elsewhere in this report, fitting slice data to an error function (representing simple Fickian diffusional transport) is controversial. Cs, Co and D obtained by this process should be regarded as fitting parameters, which may not represent the actual transport. Specifically, using such parameters to predict the future course of chloride intrusion into the structural element from which the samples were obtained may not be meaningful. Furthermore, using these results to predict chloride transport in other structural elements may be totally erroneous.

4. All entered dimensional data is converted to centimeters. The program uses millimeter resolution to evaluate the error function (tables in lower portion of spreadsheet). FITTER assumes that the data are expressed as a midpoint and thickness dimension.

5. It is quite possible that the optimal fit for Co, Cs may result in negative Co. At present the program does not preclude this possibility. It is suggested that should this occur, the program be rerun for a fixed value of Co=0 to obtain yet another interpretation of the results. FITTER is constrained to give values of Co greater than zero.

Section 4: AN ADVANCED FITTING PROCEDURE INCLUDING THE EFFECTS OF BINDING AND CARBONATION

4a Introduction

As discussed previously, it is not difficult to fit concentration data from slice specimens to the well know error function by a linear regression/optimization technique. While this approach will yield a set of D, Cs and $C_{0,}$ using this information to predict time to initiation can give erroneous results in situations where a simple Fickian model is not appropriate. Specifically situations where binding reactions are present, cylindrical and thin slab elements are tested or diffusion coefficients dependent on space or time should be modeled are much more difficult to model and fit to data. For example if significant binding is present, not only is the prediction of the location of critical concentration incorrect but also it is the free chloride (not the total concentration) that influences the onset of active corrosion. The motivation for the work in this section is a desire to estimate parameters for physical models including binding and release.

The principal complication to fitting data to a model for diffusive transport with binding is due to the fact that no analytical solution (analogous to the error function) exists to construct a basis for the regression process. There is however, another possible method of approximation that can be utilized. The approach of this method is to obtain a numerical solution to the governing differential equation, as a function of free parameters D, C_S and C_0, plus parameters describing any complicating factor (such as binding). This numerical solution can be integrated to reproduce slice data, and then optimized to give a minimal residual. It is emphasized that this fitting procedure is analogous to the conventional method involving the error function except that the underlying differential equation is used to provide a model, rather than the error function (or any other analytic function). The same technique could of course be applied to the simple Fickian model.

The purpose of this discussion is to demonstrate this approach. The methodology to extend a numerical fitting procedure to include binding is outlined below and several examples are considered. An introductory treatment of cylindrical geometries, and time dependent diffusion coefficients (no binding) has been included as a further demonstration of the method in Section 7.

The programming language utilized in this section is MATLAB, and as part of the current effort, fitting techniques for the Fickian model developed previously have also been rewritten and extended to include a general constrained optimization, which has the advantage of precluding solutions with unrealistic parameters. For example, results yielding negative background concentration can be eliminated.

4b Fitting slice data to a transport model including binding

The steps of this method are as follows:

1. The underlying differential equation describing transport in systems with equilibrium binding reactions,

$$\frac{\partial C_T}{\partial t} = \frac{\partial}{\partial x}\frac{D}{1+\frac{\partial C_B}{\partial C_F}}\frac{\partial C_T}{\partial x} \qquad 4.1$$

can be solved providing the diffusion coefficient D, the initial and background chloride ion concentration, and the isotherm parameters are all known. For the purposes of this discussion, the so-called *method of lines* (using a Gear algorithm due to a stiff system) was adopted.

2. Once a solution has been obtained, a procedure to numerically average the result over the slice dimensions is required. Here, the results were numerically interpolated and integrated using a trapezoidal scheme.

3. A residual error between the set of solution slice averages from Step 2 and actual slice data can then be constructed. Here the square of the difference was summed (unweighted) for each included slice. As discussed later, included slices may be all available data or alternatively excluding one or both of the first and last slices.

4. An inverse approach can then be adopted, seeking the set of free parameters by optimization techniques that result in a minimal residual error for the model in Step 3. A simple strategy is to adopt the surface concentration and diffusion coefficient predicted by a Fickian model, utilize the background concentration either from last slice data or from a previous modeling attempt and optimize for the parameters describing binding. A second, more complex method is to optimize for all parameters using a constrained multivariate analysis. The rationale for these choices will be further discussed below.

5. Once the unknown parameters are estimated, a (minimal error or "optimal") solution for the total and free concentration can be generated, along with a binding isotherm. This step is a major improvement over simply employing a Fickian model, since it is the critical concentration of free chlorides that determine initiation of corrosion. Assuming an equilibrium isotherm means that there is a predictable concentration of total chlorides equivalent to the critical concentration of free chlorides. Furthermore it can be shown that solutions to Equation 4.1 are similar in the parameter $x/(4Dt)^{1/2}$ (as is the error function). Thus an interpolation of the optimal solution for total chlorides will provide a penetration depth for the equivalent threshold concentration at the time of measurement. Application of the scaling parameter then will permit prediction of initiation time at any other condition without requiring another solution to the governing equation.

The method outlined above has been explored, first by developing the solution to several idealized problems (generating trial slice data), then attempting to apply the method to actual data. It is noted at the onset that usually the number of data points in a set to be fitted is small. The philosophy adopted here is to explore this technique as a possible approach to obtaining information, ignoring for the moment questions about the statistical error in fitting a model with a large number of free parameters.

4c Sample calculations

A typical example will serve to demonstrate application of this method. A concrete core specimen (porosity of 10%) having a background concentration of chlorides of 0.2 kg/m^3 is exposed on one surface to a constant environmental concentration of 200 kg/m^3 at the surface. A Langmuir equilibrium binding isotherm describes the binding reaction with k=6, C=5 and

D=4e-9 cm/sec^2 (slightly harder binding than assumed elsewhere in this report). The surface concentration including the effect of binding was taken to be 25 kg/m^3.

At age three years, the total chloride concentration in the specimen can be generated by solution to the governing differential equation as shown in Figure 1. The following slice scheme has been adopted for this example (slices start at xs and end at xf, both in cm).

```
xs=[ 0   .2    .4    .8   1.2  2.5]';
xf=[.19 .39 .79 1.19 1.59    3]';
```

Detailed (finely resolved) computed solutions can be integrated to give an average concentration, here assumed to be located at the center of the slice. These values will serve as trial data for the discussion to come and have been added to Figure 1. Note that these points do not necessarily lie on the solution curve. For comparison two error function solutions for the same D have been superposed on the graph. The difference between these solutions lies in surface concentration. First a correct surface concentration of 20 kg/m^3 was modeled, then a surface concentration of 25 kg/m^3 was imposed to simulate the naïve result of assuming that no binding is present.

The models illustrate the importance of the tail of the chloride profile. If for example, critical concentration is known to be 0.7 kg/m^3 and binding is a factor then the assumption of a Fickian model would be poor. The actual location of the critical front would be incorrectly predicted, not only because the surface concentration be affected by binding but also the modification of the profile in the crucial tail region. Furthermore, the differences between total and free chloride would not be correctly accounted for. While it is true that the Fickian projection would be conservative, a considerable benefit of binding would be ignored in estimations of service life, leading to excessive cover specifications.

It is instructive to examine the effect on the total and free chloride profiles due to variation in the two parameters k and C of the Langmuir binding isotherm. Holding C constant at a value of 5, and varying k yields the sequence of profiles shown in Figure 4.2. Figure 4.3 shows the sequence of profiles generated by maintaining k constant and varying C. In both diagrams, an expanded view of the front region is shown below the full profile. Two observations emerge. First, the variation in k causes only a small variation in the position of the front compared to variations in C. Secondly, profiles for both total and free concentration lag the Fickian model in the tail region by a considerable amount, reinforcing the discussion of service life estimation above.

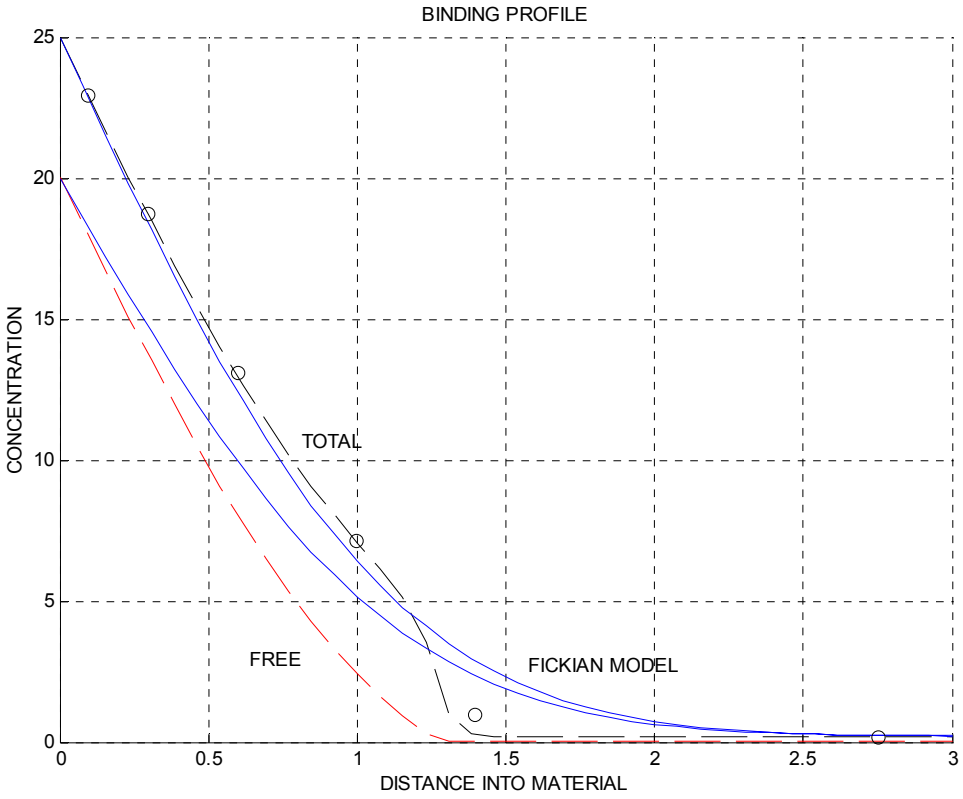

Figure 4.1 : Illustrating the solution to Equation 1 for the D=4e-9, C_S=25, C_0=0.2, k=6, C=5, Langmuir isotherm, at time three years. Symbols indicate integrated slice data from solution. Error function solutions added for comparisons. See text for units in this and subsequent figures.

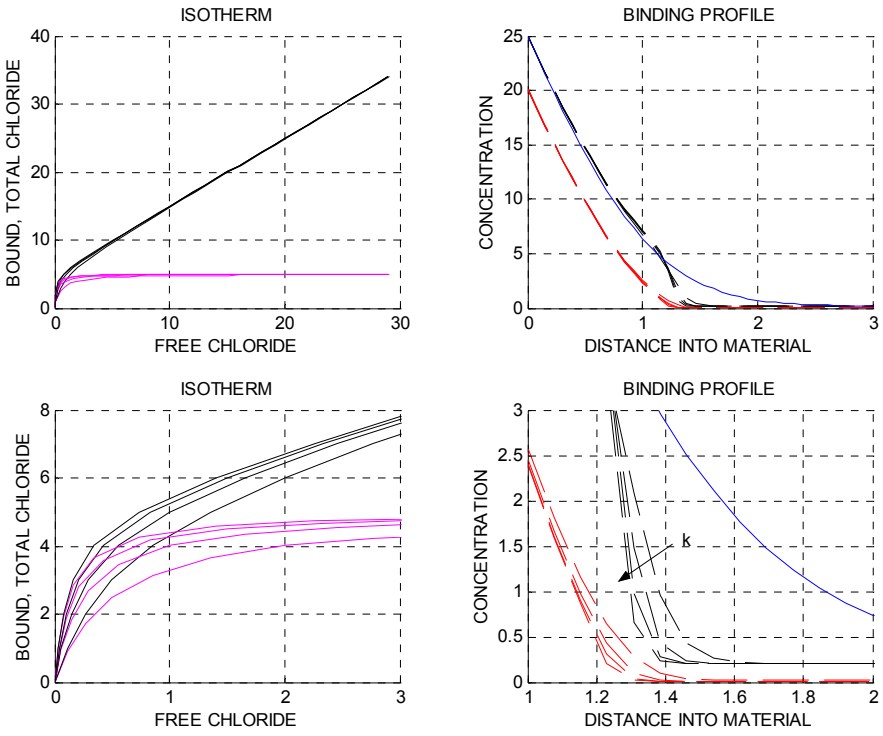

Figure 4.2: Binding models for k= 2, 4, 6, 8, while maintaining C =5.

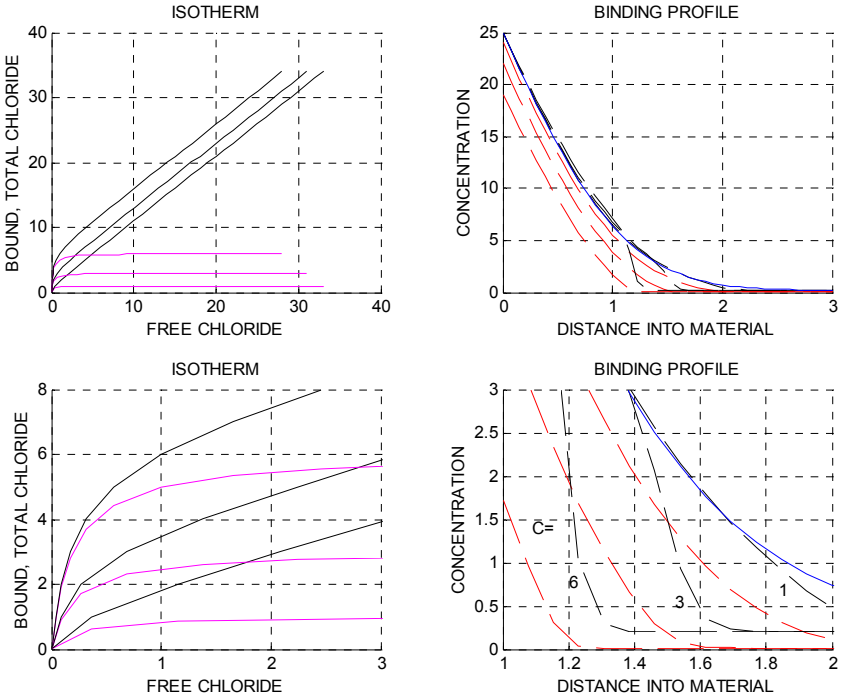

Figure 4.3: Binding models for C=1,3,6, holding k=6.

Using the method discussed earlier to produce ideal trial data for slices several additional cases have been analyzed, beginning with the data set shown in Figure 1 (which includes binding). Synthetic data generated from the total concentration profile are

```
dcl=[22.9478   18.7306   13.0873    7.1554    0.9597    0.2000];
```

for slices

```
xs=[0 .2 .4 .8 1.2 2.5]';
xf=[.19 .39 .79 1.19 1.59 3]';
```

The following upper and lower bounds on k and C were imposed

```
guess=[2;1];
ub=[guess(1)*10; guess(2)*5];
lb=[guess(1)*0; guess(2)*0];
```

A significant result is that the estimate of D is quite good even if the error function model is used (not because the error function is a good physical model but because it is a reasonably shaped basis function). For “soft” binding this result is due to the near completion of the binding reaction at a relatively low concentration, thus the rate of change of bound chlorides as a function of free chlorides is nearly zero and D is independent of binding at all except the deepest slices (providing of course that the slicing strategy closely corresponds to the actual profile). Good comparisons are not found for the estimate of (free) surface concentration due to the bound chlorides. The error function model obviously cannot provide a suitable estimate of this parameter (but can estimate the total concentration). In the final step, it is apparent that the binding parameters are successfully estimated from optimization of the solution to Equation 4.1, and a much better residual error is obtained. As is true for the error function model, a good experimental measurement of the background concentration and a reasonable estimate of the location of background can be quite helpful. It is nearly impossible to preclude a negative value from a generalized fit including background as a free parameter, reinforcing the use of experimental values for this parameter, or constraining the value to be greater than zero. Sensitivity studies are discussed elsewhere.

Even though the diffusion coefficient may be well estimated by the error function model, prediction of time to initiation is quite limited by the error introduced into the surface concentration and the failure to account for binding (results are reported for total surface concentration). Binding can alter the leading edge of the advance of chlorides into the concrete dramatically (as seen in Figure 4.1). Thus, assuming a relatively good estimate of the binding profile is generated by the fitting procedure, a prediction for initiation based on the binding model would seem to be logical.

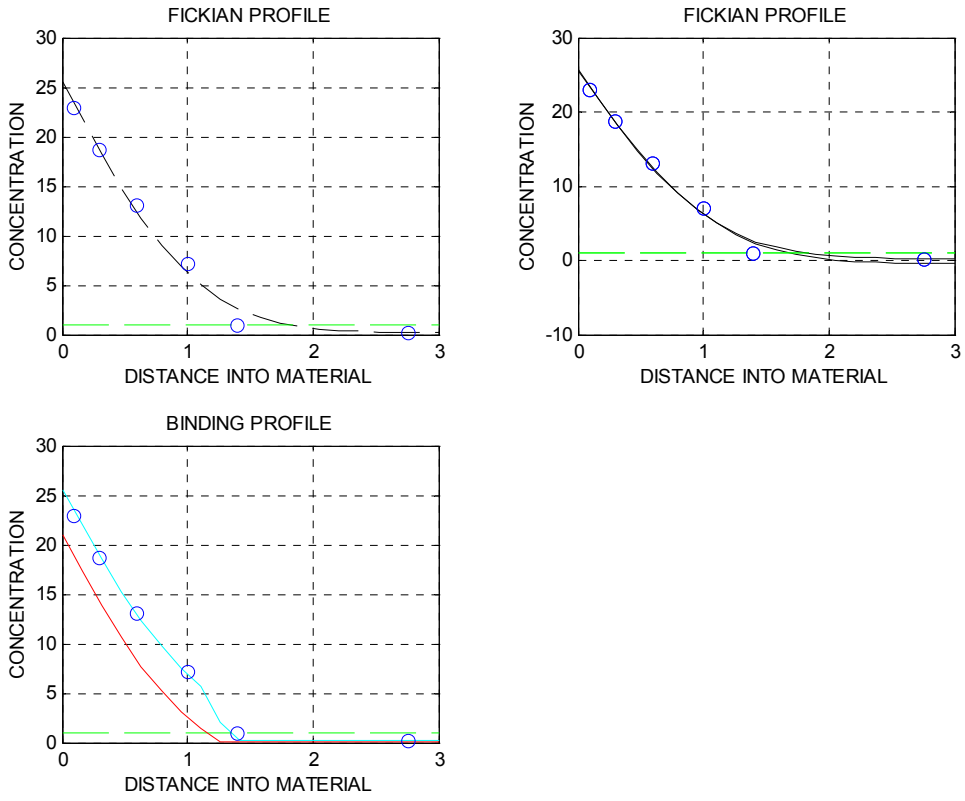

Figure 4.4: Results of data analysis for slices with binding. Top pictures are Fickian models (left represents background data, right data estimate). Lower picture shows fit to the binding model.

Program output is as follows:

Fit to Fickian profile, measured background
using all data
  Diffusion coefficient = 3.7589e-009
  Surface concentration = 25.5975
  Background concentration = 0.2
  Residual = 4.4035

Fit to Fickian profile, estimated background
using all data
  Diffusion coefficient = 4.1004e-009
  Surface concentration = 25.495
  Background concentration = -0.45502
  Residual = 3.9096

Fit to Fickian profile, estimated background
constrained optimization for D,Cs,C0
using all data
  Diffusion coefficient = 3.7453e-009
  Surface concentration = 25.6024
  Background concentration = 0.19821
  Residual = 4.402

Fit to binding profile, measured background
using all data
  Diffusion coefficient = 3.7589e-009
  Surface concentration = 25.5975
  Background concentration = 0.2
  k parameter = 6
  c parameter = 4.6957
  Residual = 0.30935

Continuing the example, the figure below shows the isotherm recovered from the fitting procedure and the projection of time to initiation for each of the models fitted to the data.

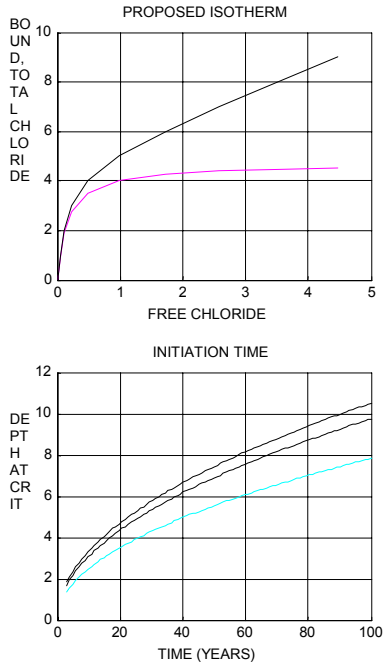

Figure 4.5: Isotherm recovered from fitting procedure (above). Projected time to initiation for a critical concentration of 0.7 kg/m^3, for all fits (below). Note improvement with binding (last curve to right).

4d Analysis of data sets with peaks

It is desirable to extend this method to situations where obvious distortions (possibly due to carbonation induced release of bound chlorides) make the top slice data not useable in the normal sense. At the initial stages of analysis, following a simple fit based on Fickian diffusion, a procedure is initiated to examine the data for evidence of distortion at the top layer. This step consists of comparing the top slice data to what would be expected from typical information. If the data does not appear to be consistent with what would be expected the top slice is ignored in the remaining computations to fit data to a binding model.

The top slice data still contains important information however. If the reason for reduced concentration in the top slice is assumed to be release of bound chlorides, then this slice is an average of a region where the total concentration is the same as the free concentration and a slightly deeper portion where the total concentration is still partially bound and partially free chlorides. These two sublayers within the top slice are separated by an interface located somewhere between the beginning and end of the slice. Once the analysis ignoring the top slice has been completed, a profile for the total and free chlorides is available. It is a relatively easy step to determine a location for the interface boundary that is consistent with the data. The program completes the modeling process by locating this interface and developing a model for the total chloride concentration extending to the surface. The importance of this reaction on the movement of the front of critical concentration is discussed elsewhere. To test the method, a second, identical set of data with the top slice altered to 20 kg/m^3 to simulate a peak was subjected to analysis.

dcl=[20 18.7306 13.0873 7.1554 0.9597 0.2000];

Results were obtained as follows:

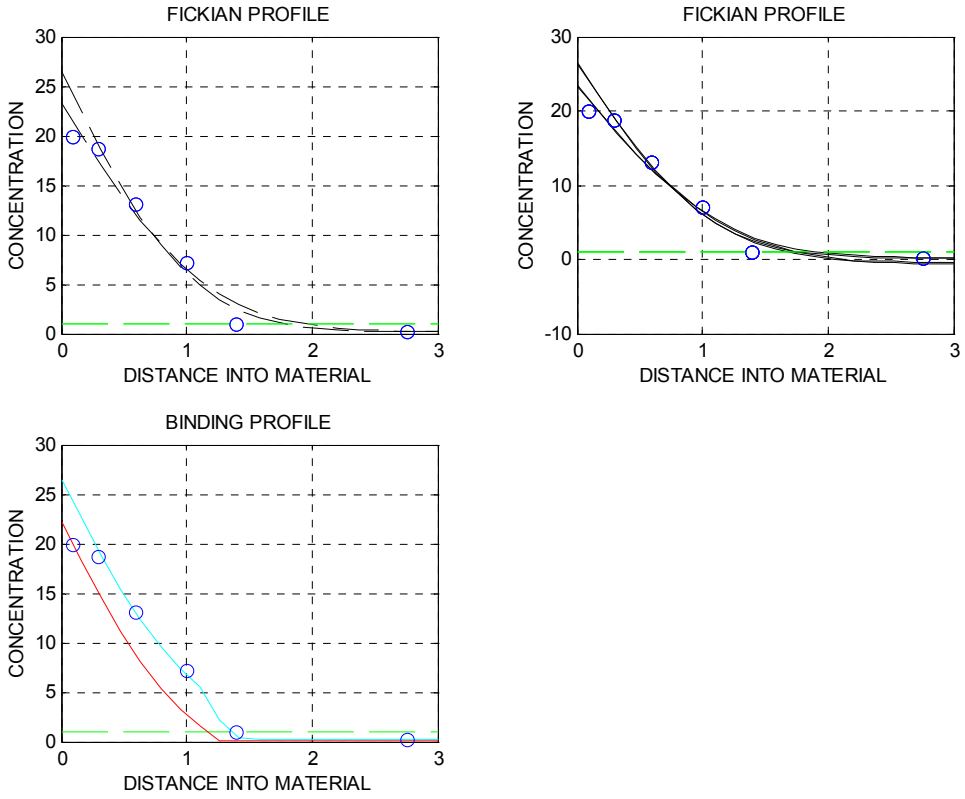

Figure 4.6: Analysis of trial data containing evidence of a peak in the first data point. All profile fits omit the top slice data.

The output of the fitting procedure is shown below. First the fitting procedure utilizes the topmost slice, then the fitting process is repeated, ignoring the first slice.

Fit to Fickian profile, measured background using all data
Diffusion coefficient = 4.3772e-009
Surface concentration = 23.3322
Background concentration = 0.2
Residual = 9.6348

Fit to Fickian profile, estimated background using all data
Diffusion coefficient = 4.9099e-009
Surface concentration = 23.2368
Background concentration = -0.65877
Residual = 8.8357

Fit to Fickian profile, estimated background constrained optimization for D,Cs,C0 using all data
Diffusion coefficient = 4.3613e-009
Surface concentration = 23.34
Background concentration = 0.19852
Residual = 9.633

PROBABLE PEAK
Repeat fit skipping first slice

Fit to Fickian profile, measured background skipping top slice due to probable peak
Diffusion coefficient = 3.5467e-009
Surface concentration = 26.5115
Background concentration = 0.2
Residual = 3.977

Fit to Fickian profile, estimated background skipping top slice due to probable peak
Diffusion coefficient = 3.8622e-009
Surface concentration = 26.2759
Background concentration = -0.3768
Residual = 3.5971

Fit to Fickian profile, estimated background constrained optimization for D,Cs,C0 skipping top slice due to probable peak
Diffusion coefficient = 3.5339e-009
Surface concentration = 26.5161
Background concentration = 0.19821
Residual = 3.9759

Fit binding profile skipping first slice: Fit to binding profile, measured background skipping top slice due to probable peak
Diffusion coefficient = 3.5467e-009
Surface concentration = 26.5115
Background concentration = 0.2
k parameter = 5.9976
c parameter = 4.3708
Residual = 0.56032
Flag = 1

When including the top slice data, results obtained for the transport parameters are reasonable but accompanied by a relatively high residual error. The fitted parameters are much improved by skipping the top slice, and are very good when including the effect of binding. It is emphasized again that these trial data are “ideal” and not contaminated by experimental error.

Finally, the program makes an effort to utilize the top slice data and project the position of a carbonation front that would give equivalent data. This location is determined by an optimized fit also, assuming that all the bound chlorides are released:

Profile with release, measured background
Interface estimated at 0.18322
Top slice data = 20
Estimated slice concentration = 19.9997

Thus the profile drops from the apparent total to the free concentration, a quantity approximately equal to the factor C. The final profile estimate is included in Figure 7, lower right frame. The indicated free surface concentration is higher than the actual value of 20 kg/m^3. This information could easily be used to develop a better estimate yet of all transport parameters, by refitting the data using a better starting value. This step could become the basis for an iterative improvement algorithm. It is also noted that the rate of carbonation could be estimated from the position of the reaction front.

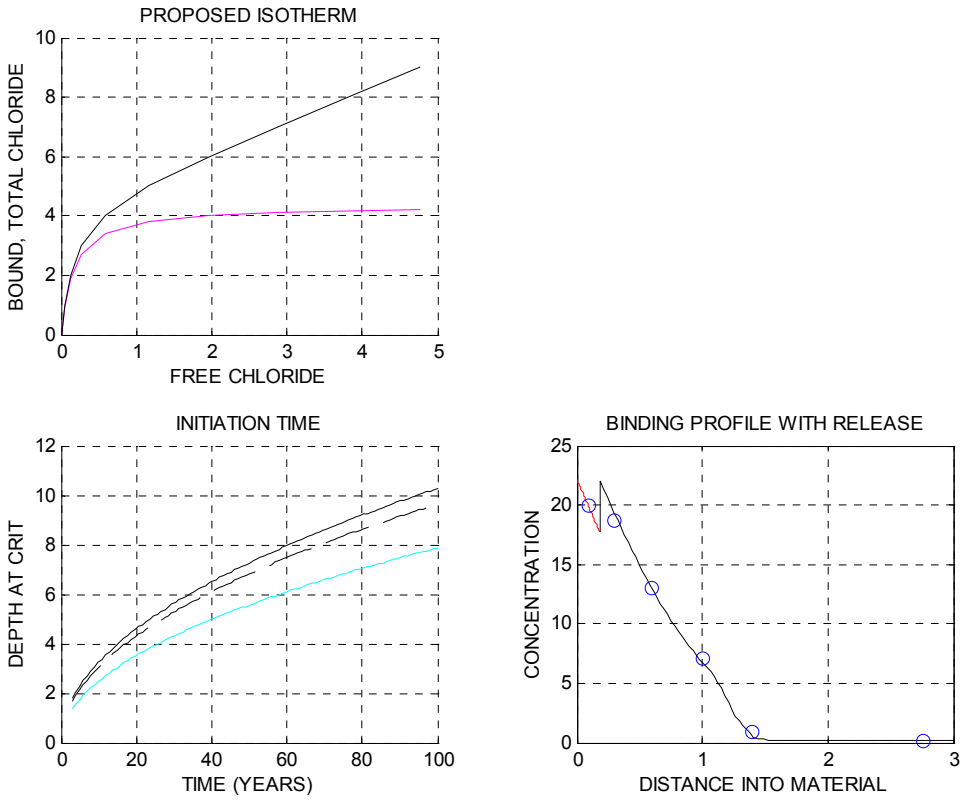

Figure 4.7. Showing the recovered isotherm, the projected time to initiation and at lower right, the proposed profile, best fitting the data slices, using a binding release model to account for the top slice data.

4e Fitting a simple diffusion case

Using the same slicing scheme as in the previous discussion, a set of trial data was generated for a surface layer concentration of 20 kg/m^3 and no binding reaction.

dcl=[18.2817 14.7540 10.0528 5.2827 2.4134 0.2359];

The purpose of investigating this case was to determine what results would be obtained if a specimen having no binding reaction was analyzed assuming that some binding might be present. Results were obtained as follows:

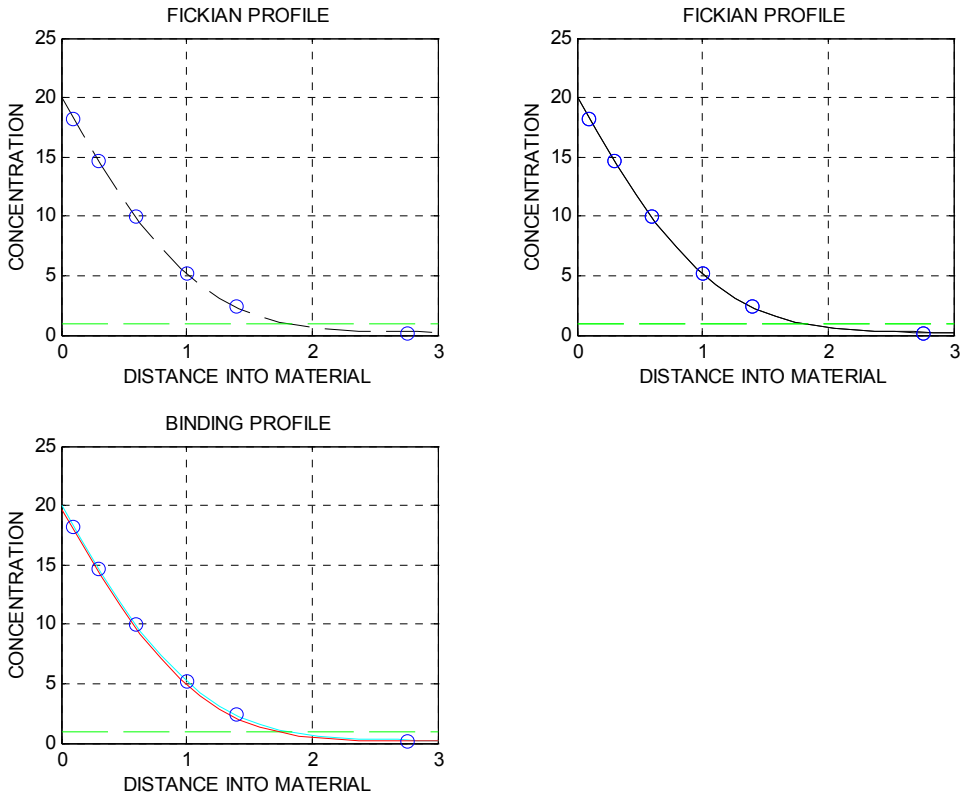

Figure 4.8. Analysis of a data set not including binding reaction.

Fit to Fickian profile, measured background
using all data
  Diffusion coefficient = 3.9731e-009
  Surface concentration = 20.0077
  Background concentration = 0.2359
  Residual = 0.0013548

Fit to Fickian profile, estimated background
using all data
  Diffusion coefficient = 3.9999e-009
  Surface concentration = 20
  Background concentration = 0.20004
  Residual = 5.275e-009

Fit to Fickian profile, estimated background
constrained optimization for D,Cs,C0
using all data
  Diffusion coefficient = 3.9752e-009
  Surface concentration = 20.0011
  Background concentration = 0.22038
  Residual = 0.00088216

Fit binding profile using all data

Fit to binding profile, measured background
using all data
  Diffusion coefficient = 3.9731e-009
  Surface concentration = 20.0077
  Background concentration = 0.2359
  k parameter = 1.4916
  c parameter = 0.32808
  Residual = 0.001121

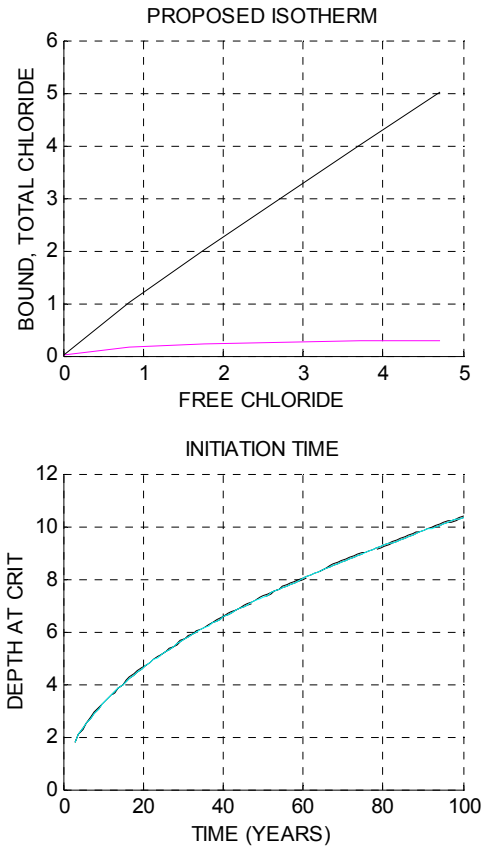

Figure 4.9: Projections for the simple diffusional case

It is evident that the first component of the program does successfully fit the slice data to an error function model as would be expected. Both efforts to fit the data with a binding model resulted in reasonable assessments of D and the background concentration. The binding parameters k and C were estimated to be relatively small, and show little variation from the model without binding.

4f Analysis of field data using the proposed method

As a first effort to apply the method discussed above to field data, a series of six tests from cores extracted from the Sunshine Skyway Bridge were analyzed. Data were as follows (distances in the table are in inches, concentrations in table and results in lb/cu.yd.; diffusion coefficients in the results are expressed in cm^2/sec):

		Core #	1	2	3	4	5	6
Start	End	Mid	SSK117-2	SSK10-16	SSK10-16	SSK116	SSK116	SSK116
0	0.25	0.125	27.43	32.41	32.14	32.14	20.98	31.85
0.25	0.5	0.375	8.23	13.61	15.16	14.66	10.54	18.46
0.5	1	0.75	0.55	3.88	4.55	7.65	5.17	11.22
1	2	1.5	0.08	0.14	0.14	0.29	0.57	1.24
2	3	2.5	0.11	0.1	0.15	0.12	0.13	0.36

Specimen SSK116 (Core #4) yielded the following results:

Fit to Fickian profile, measured background
using all data
  Diffusion coefficient = 7.4954e-009
  Surface concentration = 39.4517
  Background concentration = 0.12
  Residual = 12.7847

Fit to Fickian profile, estimated background
using all data
  Diffusion coefficient = 6.8942e-009
  Surface concentration = 39.8607
  Background concentration = 0.71097
  Residual = 12.1728

Fit to Fickian profile, estimated background
constrained optimization for D,Cs,C0
using all data
  Diffusion coefficient = 7.4098e-009
  Surface concentration = 39.4518
  Background concentration = 0.1294
  Residual = 12.7796

Fit binding profile using all data

Fit to binding profile, measured background using all data

Diffusion coefficient = 7.4954e-009
Surface concentration = 39.4517
Background concentration = 0.12
k parameter = 6
c parameter = 1.0852

Residual =12.1432

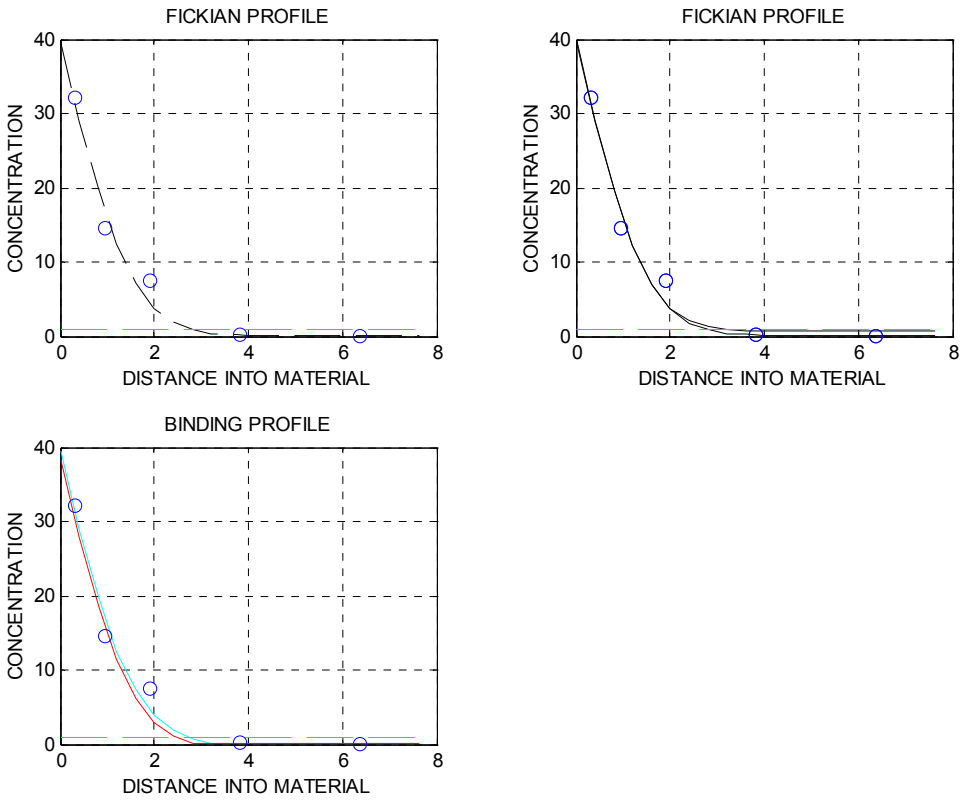

Figure 4.10 Fit to field data, core #4.

The remainder of the testing produced the following results

Core 1

Fit to Fickian profile, measured background
using all data
  Diffusion coefficient = 8.0884e-010
  Surface concentration = 41.0906
  Background concentration = 0.11
  Residual = 0.069327
    0.0040

Fit to Fickian profile, estimated background
using all data
  Diffusion coefficient = 8.1835e-010
  Surface concentration = 41.0256
  Background concentration = 0.020554
  Residual = 0.048505

Fit to Fickian profile, estimated background
constrained optimization for D,Cs,C0
using all data
  Diffusion coefficient = 8.0886e-010
  Surface concentration = 41.0907
  Background concentration = 0.10984
  Residual = 0.069254

Fit binding profile using all data

Fit to binding profile, measured background
using all data
  Diffusion coefficient = 8.0884e-010
  Surface concentration = 41.0906
  Background concentration = 0.11
  k parameter = 0.32769
  c parameter = 4.783
  Residual = 0.0094524

Core 2

Fit to Fickian profile, measured background
using all data
  Diffusion coefficient = 1.4471e-009
  Surface concentration = 43.2657
  Background concentration = 0.1
  Residual = 1.6016

Fit to Fickian profile, estimated background
using all data
  Diffusion coefficient = 1.3963e-009
  Surface concentration = 43.4556
  Background concentration = 0.39664
  Residual = 1.4114

Fit to Fickian profile, estimated background
constrained optimization for D,Cs,C0
using all data
  Diffusion coefficient = 1.444e-009
  Surface concentration = 43.267
  Background concentration = 0.10115
  Residual = 1.6007

Fit binding profile using all data

Fit to binding profile, measured background
using all data
  Diffusion coefficient = 1.4471e-009
  Surface concentration = 43.2657
  Background concentration = 0.1
  k parameter = 2.1627
  c parameter = 0
  Residual = 1.3126

Core 3

Fit to Fickian profile, measured background
using all data
  Diffusion coefficient = 1.7712e-009
  Surface concentration = 41.6176
  Background concentration = 0.15
  Residual = 0.84314

Fit to Fickian profile, estimated background
using all data
  Diffusion coefficient = 1.7437e-009
  Surface concentration = 41.6899
  Background concentration = 0.28304
  Residual = 0.80708

Fit to Fickian profile, estimated background
constrained optimization for D,Cs,C0
using all data
  Diffusion coefficient = 1.7692e-009
  Surface concentration = 41.6176
  Background concentration = 0.15087
  Residual = 0.84284

Fit binding profile using all data

Fit to binding profile, measured background
using all data
  Diffusion coefficient = 1.7712e-009
  Surface concentration = 41.6176
  Background concentration = 0.15
  k parameter = 2.1354
  c parameter = 0
  Residual = 0.68138

Core 4

Fit to Fickian profile, measured background
using all data
  Diffusion coefficient = 2.2487e-009
  Surface concentration = 39.4515
  Background concentration = 0.12
  Residual = 12.7847

Fit to Fickian profile, estimated background
using all data
  Diffusion coefficient = 2.0683e-009
  Surface concentration = 39.8605
  Background concentration = 0.71089
  Residual = 12.1728

Fit to Fickian profile, estimated background
constrained optimization for D,Cs,C0
using all data
  Diffusion coefficient = 2.223e-009
  Surface concentration = 39.4515
  Background concentration = 0.1293
  Residual = 12.7798

Fit binding profile using all data

Fit to binding profile, measured background
using all data
  Diffusion coefficient = 2.2487e-009
  Surface concentration = 39.4515
  Background concentration = 0.12
  k parameter = 2.222
  c parameter = 1.0011
  Residual = 12.3148

Core 5

Fit to Fickian profile, measured background
using all data
  Diffusion coefficient = 2.6042e-009
  Surface concentration = 25.3786
  Background concentration = 0.13
  Residual = 3.2377

Fit to Fickian profile, estimated background
using all data
  Diffusion coefficient = 2.4187e-009
  Surface concentration = 25.5865
  Background concentration = 0.49614
  Residual = 3.0067

Fit to Fickian profile, estimated background
constrained optimization for D,Cs,C0
using all data
  Diffusion coefficient = 2.579e-009
  Surface concentration = 25.3787
  Background concentration = 0.13631
  Residual = 3.2341

Fit binding profile using all data

Fit to binding profile, measured background
using all data
  Diffusion coefficient = 2.6042e-009
  Surface concentration = 25.3786
  Background concentration = 0.13
  k parameter = 2.2808
  c parameter = 0.0044165
  Residual = 3.0961

Core 6

Fit to Fickian profile, measured background
using all data
  Diffusion coefficient = 4.2395e-009
  Surface concentration = 36.4004
  Background concentration = 0.36
  Residual = 8.4764

Fit to Fickian profile, estimated background
using all data
  Diffusion coefficient = 4.2004e-009
  Surface concentration = 36.4307
  Background concentration = 0.43366
  Residual = 8.4687

Fit to Fickian profile, estimated background
constrained optimization for D,Cs,C0
using all data
  Diffusion coefficient = 4.2325e-009
  Surface concentration = 36.4004
  Background concentration = 0.36331
  Residual = 8.4759

Fit binding profile using all data

Fit to binding profile, measured background
using all data
  Diffusion coefficient = 4.2395e-009
  Surface concentration = 36.4004
  Background concentration = 0.36
  k parameter = 2.5669
  c parameter = 2.5425
  Residual = 8.2095

4g Conclusions regarding the use of advanced modeling

1. An advanced approach to fitting experimental slice data to a binding model has been developed. The basis of this method is a numerically generated solution to the differential equation describing binding. The difference between slice integrated averages for this detailed solution and the actual experimental data is minimized in the least square error sense. This inverse process involves many recomputations of the profile solution to optimize the set of descriptive parameters.

2. An operational program to construct fits to experimental data using both an error function model and a binding model has been developed and tested both with simulated data and real experimental data from the field.

3. Limitations of the simple Fickian approach to computing time to initiation have been examined. Based on the simulated slice analyses, it appears that the assumption of binding may be better initially, even if the results eventually return parameters more consistent with simple Fickian diffusion. This is because Fickian diffusion is a special case of binding and the method discussed here can reveal that fact.

4. The method discussed here has been extended to the case of inconsistent top slice data. The fitting procedure incorporates a scheme for ignoring the top slice data, and then later examines for the possible penetration of a front of released bound chlorides.

Section 5: STRATEGY FOR SELECTING SLICE DIMENSIONS AND ANALYSIS OF DATA

5a Strategy for conventional analysis

The following strategy for choosing appropriate slice dimensions for a core specimen is suggested, based on the results of the results of this investigation.

Step 1: Summarize known information: Salinity, location AHT, estimates of C_S, C_0 (State limits provide a guide), type and mix of concrete, age (to tenths of years), and the critical concentration for initiation. Examine the core for cracks. Use the **Time to Initiation** program developed for FDOT under a previous project [4] or a similar algorithm to obtain preliminary estimates of diffusion coefficients, and surface concentration in the absence of other information. The time to initiation predicted by this program may also be useful for general comparisons but is clearly not on the same footing with eventual core specific predictions.

At present, typical values for parameters of interest are as follows:

Surface concentration (in concrete, assuming a porosity of 10%)	
Chloride saturated	25kg/m^3
Typical marine	5 kg/m^3
Background concentration	
minimum	0 kg/m^3
typical	0.1 kg/m^3
Diffusion Coefficient	
high quality	1e-9 cm^2/s
medium-low quality	<1e-8 cm^2/s
Binding constant	
estimate	2 kg/m^3
Binding coefficient	2 m^3/kg
Critical concentration (conservative)	0.7 kg/m^3

The depth at which the critical concentration is located plus the transport parameters listed above determine the time to initiation (critical concentration at rebar depth). Figure 5.1 shows the core specimen and important time and space relationships.

Step 2: Determine slice position and dimensions. The problem of determining how to slice the concrete core specimen reduces to optimizing the cuts to obtain the maximum amount of information from the data. It is likely that the cost of slicing the specimen is small in comparison to analyzing any particular slice. The following example assumes that six total slices are economically justified; obviously more slices will produce better results.

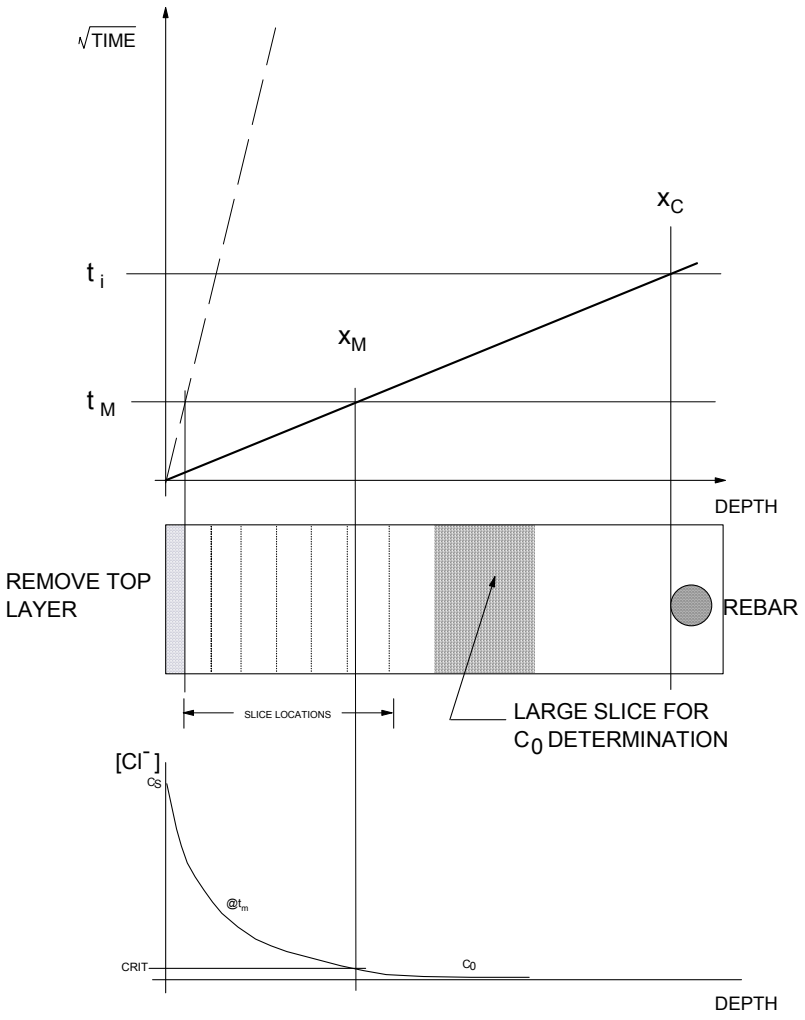

Figure 5.1: Relationship between slice locations and deduced parameters.

Assuming the background concentration is about 1% of the surface concentration, an approximate minimum start for a slice to determine the background can be obtained from the following formula (units must be consistent):

$$x_{1\%} = 3.64\sqrt{Dt_m} \qquad 5.1$$

The same approach may be used to estimate the thickness of a carbonated front

$$x_{carb} = R\sqrt{t_m} \qquad 5.2$$

.

These two formulas may be used to judge how slicing should proceed. For example, if the diffusion coefficient is estimated to be 1e-8 cm^2/sec and the time of coring, t_m, is 10 years (3e8 sec), Dt =3 and the 1% error value is 6.3 cm which indicates the starting depth for a broad cut for C_0 determination. Note that a conservative value for D should be selected to ensure a true background is obtained. A slice of 1 cm or more is suggested.

Typical values for R range from ~0 to 0.5cm/$yr^{1/2}$ [22]. Assuming a value of 0.1 cm/$year^{.5}$ for R, the top slice for this example would be about 0.3 cm thick. Again, a generous slice is probably a better choice since fitting techniques assume the carbonation does not extend beyond the first slice. The core region remaining then extends from 0.3 cm to about 6.3 cm (in some cases such as a young specimen of dense concrete the actual remaining sample could be quite small). Depending on the method used to cut the slices (lathe or saw) as many specimen slices as possible should be cut. The thickness of a cut will be limited by saw kerfs, dimensional accuracy, and ensuring that a representative sample is obtained. For saw cutting, specimens as small as 3 mm thick may be possible. For all slices, start and finish dimensions should be recorded (accounting for any saw kerfs).

Step 3: Analyze slice specimens for total chloride content, beginning with the background slice. If the background concentration obtained is higher than the State design limits or the critical concentration level, the presence of a crack in the specimen is possible [4]. The testing should be reconsidered at this point. The order in which the remaining specimens are analyzed is important to minimize costs. Ignoring for the moment the top slice, analyze the second slice from the surface. A specimen from the middle of the sample should be analyzed next (for this example located at about 3.3 cm). If this sample does not exhibit a concentration at least as large as the critical, then all deeper slices will not yield much new information and are likely to be unprofitable. If this were the case, then the next slice would be chosen about half way between the center and the second slice from the surface. At this point, a partial profile can be constructed with four points and judgment can be exercised as to how to select the remaining slices to analyze. As many specimens as can be economically justified should be obtained. The top slice may provide significant information about the possible presence of binding reactions as well as carbonation. Developing information about the apparent location of the critical concentration is extremely important. If binding reactions are present then distortion of the profile occurs for concentrations in the tail region, but the actual free concentration will attain the critical level at some reduced depth.

Returning to an early step, if analysis of the center specimen yields a concentration significantly higher than critical, simply bisecting the deeper half to obtain more of the profile may be a poor choice, depending on how many specimens exist. The best choice may be inferred by examining the partial profile, perhaps even developing a preliminary Fickian fit.

Step 4: When analysis is complete, plot slice data (at mid points) looking for obvious features. Does the profile show a peak or bulge? What is the value of C_o measured? Is this value greater than the critical concentration or greater than State limits? Where is the center of this slice with respect to the reinforcing depth? If the background estimate is found to exceed the State mandated limits, or the critical concentration (especially if located near the rebar) further analysis may not be profitable. The core may have come from cracked concrete.

Step 5. If the data set passes the scrutiny outlined in previous steps, fit using either FITTER (simple error function fit) to obtain C_o, C_S, and D. Examine correlation (residual error and

Pearson's R) between the data and fit. This qualitative comparison only indicates how well the data fit the model. Correctness of the model is not proven.

Step 6. For simple error function models a forecast of time to initiation can be made directly. Some judgment will be needed in order to assess the value of the core information. Possible conclusions are

a. All methods give similar results and a good fit correlation is obtained. The data and the fits are not suspect in any way. The time of initiation can be estimated. Further analysis will be required to estimate the error bounds on the prediction.

b. High concentrations of chloride apparently exist in the background, possibly near the rebar at the time of testing. It is likely that the core came from cracked concrete or corrosion has already begun. Further analysis will probably not yield useful information.

c. The first data set is insufficient or flawed in some manner. Predictions are not worthwhile and it may be necessary to utilize additional slice specimens performing the same analysis steps again (using more slice data) to produce valid results.

d. As a final step the initial assumptions about slicing and carbonation should be checked. It may be worth sampling the top slice for carbonation.

5b A cutting strategy for critical front measurement

As pointed out in Section 3, an alternative method to determining effective diffusion parameters is to attempt to locate the position of the critical concentration threshold at the time of coring and use this data to compute a time to initiation. This approach recognizes that the true goal is to predict time to initiation and not to validate any particular model. Accordingly, the ideal strategy is to estimate the approximate position of this front then concentrate all slicing in this area. Several procedures could then be used to fit the data to arbitrary models to determine the location of the front.

In situations where binding is known to be active, the critical concentration in free chlorides could be used to calculate an equivalent total chloride concentration.

5c Variation of cutting location to optimize parameters

It is desired to minimize the error between C_{Sest} and $C_{Sactual}$ and similarly for D. The objective of the work reported here was to determine if the slice positioning has any significant effect on the values of Cs and D for realistic data sets (ie error contaminated). Consider the previously derived expression

$$C_S = \frac{\sum_i C_i \varphi_{1i} - C_0 \sum_i \varphi_{1i}\varphi_{2i}}{\sum_i \varphi_{1i}^2} \qquad 5.3$$

with the identity

$$\varphi_{1i} = 1 - \varphi_{2i} \qquad 5.4$$

Here C_i are real data, and the net effect of changing the slice positioning is to change the values of the φ_i. In principle the value of Cs predicted could be affected by this choice.

A program was constructed to determine the residual error between predicted parameters and ideal parameters for variable slice positions. The profiles tested were obtained by integrating (over the slice dimension) the ideal concentration profile, then adding a fixed error term during the optimization procedure. It is noted that this is only one of several possible interpretations. The residuals were developed for the position of the critical front, the diffusion coefficient and the surface concentration. At this time no particular cutting strategies were found to give better results than others, thus no particular strategy can be recommended. This issue could be revisited at a later date however.

Section 6: CORROSION INITIATION TIME DERATING FACTORS FOR REBARS IN CONCRETE INCLUDING GEOMETRICAL EFFECTS

Outline

Buildup of chlorides in the region of a rebar have been discussed previously for planar geometry [4,23]. Here, further efforts have been made to understand the influence of rebar positioned near an exterior corner and rebar lap joints. In the case of a rebar located along a 45^{o} line from an exterior corner, the simultaneous effect of acceleration of chloride penetration due to the two sided corner in combination with the accumulation due to the rebar produces a marked decrease in the time to initiation of corrosion. When two bars are located side by side to form a splice, again a more rapid buildup occurs than would be expected for the planar case of a single rebar, due to the larger projected area. Derating factors are calculated and results are compared to the simple planar geometry for both cases.

Introduction

Rebar embedded in concrete structural elements exposed to environmental chloride ions (eg. marine service, deicing salts) is subject to depassivation as these ions are transported to the steel-concrete interface. In conventional design calculations, extremely simple transport models (one dimensional Fickian diffusion employing an effective diffusion coefficient) are utilized to estimate of the growth of chloride concentration at the cover depth. Computational modeling has been used however, to demonstrate [23] that a rapid buildup of chloride concentration may be induced in the region just in front of the rebar (on the side facing the exposed concrete surface) due to the local obstruction to chloride transport by the impermeable metal. If the concentration were to rise faster at this location than that rate which would be expected if no rebar was present, this effect could be of considerable importance for the selection of concrete cover in the design of concrete structures. Failure to account properly for this effect could lead to a shortening of the service life of the structure, since typically the time to initiation is a large fraction of the total period.

A derating factor T_f has been defined as the ratio of the time to initiation for the two dimensional problem to the time to initiation using the one dimensional (error function) solution to Fick's second law (Equation 3.1). Estimates of this derating correction factor as a function of the ratio of rebar diameter to clear cover and the ratio of critical concentration for corrosion initiation to surface concentration of chloride ions were presented in [23].

In addition to evaluating the derating factor, another very significant result of this work was to quantify the decrease in time to initiate corrosion, t_i , with increasing threshold concentration. Thus the derating factor becomes smaller as the threshold concentration is elevated and anticipated benefit may be lost if an inhibitor is employed to compensate for a reduced cover dimension.

Only simple diffusion was considered in References [4,23] and the problem was modeled using Fick's second law in two dimensions. The assumption of pure diffusion as the transport mechanism for chloride ions may well be overly simplistic. In addition to moisture transport, physical and chemical binding reactions may influence the evolution of chloride concentration in the concrete. A tacit assumption is that the time derating factor will be approximately independent of the transport mechanism (including binding effects. While it may be argued that aggregate exerts a similar effect on the transport of chlorides and may actually shield the rebar to some extent, a more conservative approach is to assume that transport to the cover depth is unimpeded and governed by an effective diffusion coefficient.

Only the case of a single rebar embedded in a semi-infinite slab has been considered to date. The purpose of the present Section is to amplify and extend the results of Ref [23] to two other geometries of interest to the designer, rebar located in proximity to a corner and two rebars located side by side as in a splice situation (Figure 6.1).

Analysis

The method of analysis used here follows closely that of References [4,23]. Fick's Second Law was solved by a simple central difference-forward time scheme with equal incremental spacing in both dimensions. As shown in Figure 6.1, Case A, the rebar was approximated as an octagonal shape, with an effective diameter, φ (maximum transverse dimension), of sixteen grid increments. The clear cover, X_c was defined as the distance from the leading rebar face to the exposed surface of the concrete. Computations for the semi infinite slab were extended to smaller values of the ratio of φ/X_c, as shown in Figure 2. In the limit of large cover to diameter ratio, the derating approaches the case of a slab of finite thickness with the back wall insulated.

Similar computations were made for the case of a single rebar located near a corner (both faces exposed to a constant chloride concentration), along a 45E line from the corner as shown in Figure 1, Case B. The diameter to cover ratio was defined as before. Computations show that for low ratio of critical to surface concentration (C_T/C_S) and large diameter to cover ratio the point on the surface developing the highest concentration (and therefore the earliest initiation) faces the exposed surfaces. For higher values of both ratios, the point of highest concentration moves towards the point lying along the 45^o line from the corner. Thus, to develop a derating factor corresponding to the planar case, the point of highest concentration was always selected to as the earliest initiation of corrosion, but in calculating the derating factor the

time to initiation based on the error function was calculated based on the clear cover dimension. The derating factor computed in this manner is illustrated in Figure 3 as a function of the diameter ratio and the concentration ratio. For large values of the diameter to cover ratio, the derating would be expected to approach the case of an insulated wall as discussed previously (indicated limiting values). At the other extreme of small diameter to cover, the derating approaches the case of derating for a corner with no rebar present, a point located on the diagonal as treated in Ref [24].

Another case of interest concerns the possibility of even more rapid buildup of chlorides induced when rebars are located in close proximity to one another so that mutual influence is felt. Such a situation commonly occurs when rebar is spliced, by placing bars side-by-side (Figure 1 Case C). Numerical experiments show that the rebar must be spaced closer than about one diameter for a substantial effect. Thus side-by-side rebar spacing at connections warrants investigation. Derating factors were obtained for two adjacent octagons, by the same approach used previously. Results are shown in Figure 4. As in the case of corner geometry, the point of earliest concentration development is not fixed, but rather moves from the leading face down into the cavity formed between the two rebars at the center. In the limit of large diameter to cover ratio it is expected that the derating curves would approach values for the case of an insulated wall as explained previously.

In addition to the working graphs shown in Figures 2-4, the coordinates used to plot these graphs are summarized in Table 1, so that interpolation in two variables can be used to predict derating over the entire interval (0#φ/X_c,$1, 0.05 #$C_T/C_S$ $ 0.5) considered here.

Conclusions

The computational results of the investigation showed that:

1. The time to corrosion initiation for rebars located near corners was reduced substantially compared to a case of a single rebar embedded in a semi-infinite slab. This effect was found to be larger as the ratio of critical concentration to surface concentration increased. For this case, the limiting value for small diameter to cover ratio is not unity.

2. Side-by-side rebar splices resulted in further reduction in the derating factor beyond the single rebar configuration.

Table 1: Time derating factors for Cases A, B and C presented as coordinates for purposes of interpolation. Ranges $0 \# \varphi/X_c, \$1$, $0.05 \# C_T/C_S \$ 0.5$

PLANAR GEOMETRY -SINGLE REBAR						
φ/Xc	**R=0.05**	**0.1**	**0.2**	**0.3**	**0.4**	**0.5**
1.00	0.78	0.73	0.65	0.58	0.52	0.45
0.94	0.78	0.73	0.65	0.59	0.52	0.46
0.80	0.78	0.74	0.67	0.60	0.54	0.48
0.53	0.80	0.76	0.70	0.65	0.60	0.56
0.40	0.81	0.78	0.73	0.69	0.66	0.64
0.27	0.84	0.81	0.78	0.75	0.74	0.73
0.16	0.87	0.86	0.84	0.84	0.83	0.83
0.00	1.00	1.00	1.00	1.00	1.00	1.00

CORNER GEOMETRY-SINGLE REBAR						
φ/Xc	**R=0.05**	**0.1**	**0.2**	**0.3**	**0.4**	**0.5**
1.00	0.77	0.70	0.59	0.50	0.41	0.32
0.94	0.77	0.70	0.59	0.49	0.41	0.32
0.80	0.76	0.69	0.58	0.49	0.40	0.32
0.64	0.75	0.68	0.57	0.48	0.40	0.32
0.53	0.74	0.67	0.56	0.48	0.40	0.32
0.40	0.73	0.66	0.56	0.48	0.40	0.33
0.27	0.72	0.66	0.56	0.49	0.42	0.35
0.16	0.72	0.66	0.58	0.50	0.44	0.37
0.08	0.74	0.68	0.60	0.53	0.46	0.39
0.00	0.77	0.71	0.63	0.55	0.48	0.41

PLANAR GEOMETRY -TWO REBAR SPLICE						
φ/Xc	**R=0.05**	**0.1**	**0.2**	**0.3**	**0.4**	**0.5**
1.00	0.78	0.73	0.64	0.57	0.49	0.40
0.94	0.78	0.73	0.65	0.57	0.49	0.40
0.80	0.78	0.73	0.65	0.57	0.49	0.40
0.64	0.79	0.74	0.66	0.58	0.50	0.41
0.53	0.79	0.74	0.66	0.58	0.50	0.43
0.40	0.80	0.75	0.67	0.59	0.53	0.46
0.27	0.81	0.76	0.69	0.63	0.59	0.55
0.16	0.83	0.79	0.75	0.72	0.69	0.68
0.08	0.87	0.85	0.84	0.83	0.83	0.83
0.00	1.00	1.00	1.00	1.00	1.00	1.00

Case A

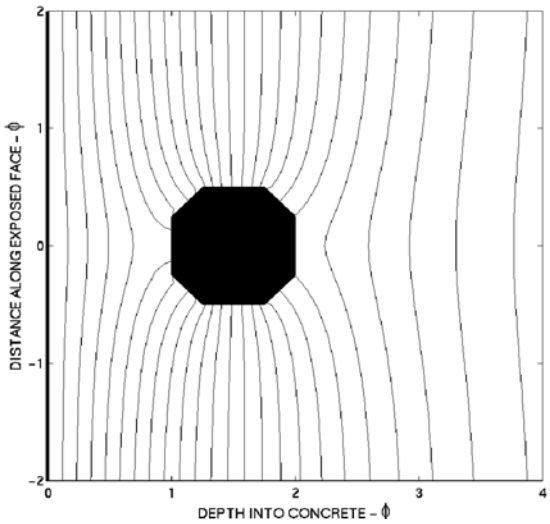

Case B

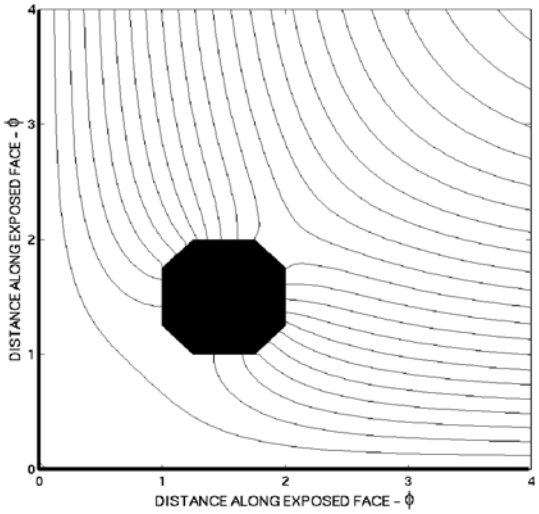

Case C

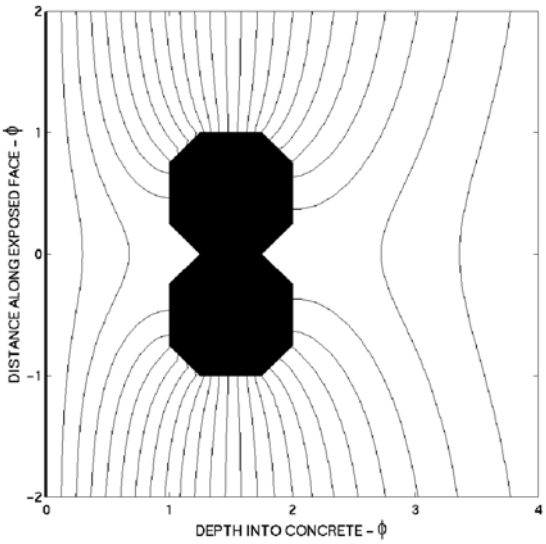

Figure 6.1 Arrangement of rebar in concrete for three cases at 1e9 seconds (Case A: single rebar, semi-infinite slab; Case B: single rebar at corner; Case C: two rebar splice in semi-infinite slab). Diameter to cover ratio equals one and =.3162. Contours are spaced at intervals of 0.04 C_S.

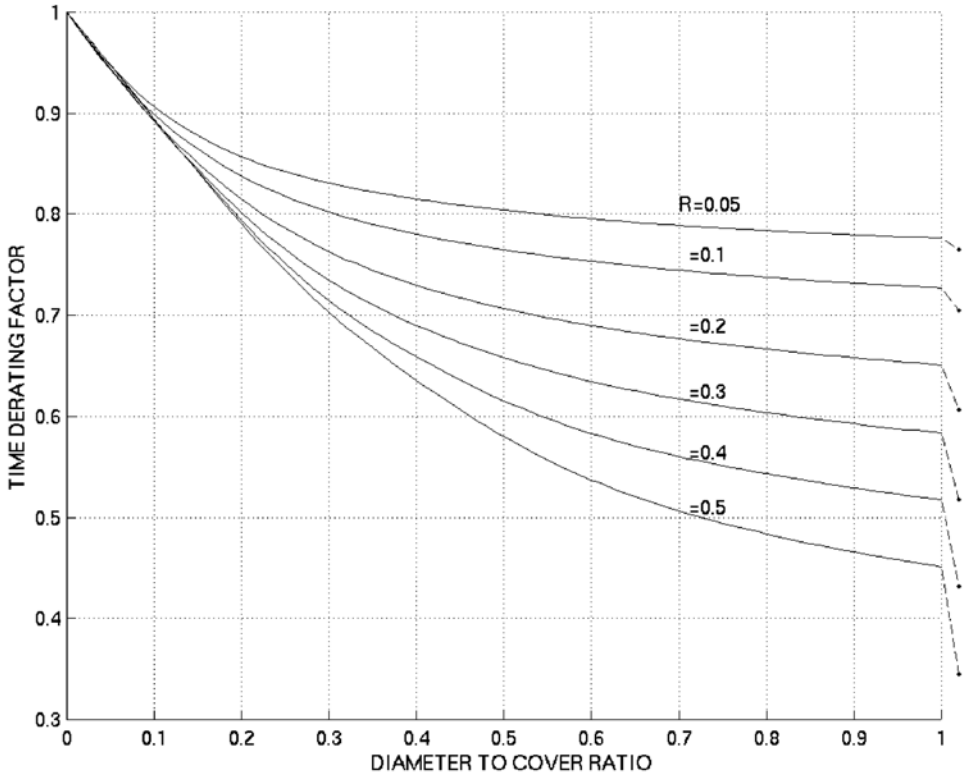

Figure 6.2: Derating factors for single rebar, semi-infinite geometry (Case A) as a function of the rebar to cover ratio Φ/X_c, and $R=C_T/C_S$ the critical concentration ratio. Limiting case for infinite cover ratio shown at right side of graph.

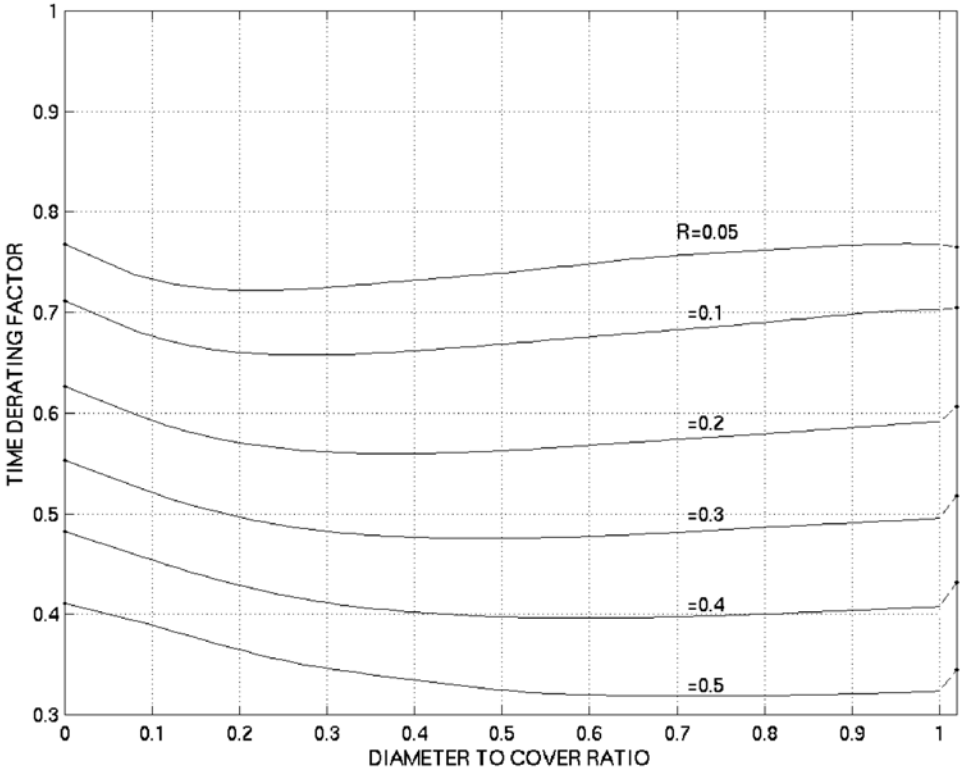

Figure 6.3: Derating factors for single rebar, corner geometry (Case B) as a function of the rebar to cover ratio Φ/X_c, and $R=C_T/C_S$ the critical concentration ratio. Limiting case for infinite cover ratio shown at right side of graph. Limiting case for vanishingly small cover ratio shown at left side of graph.

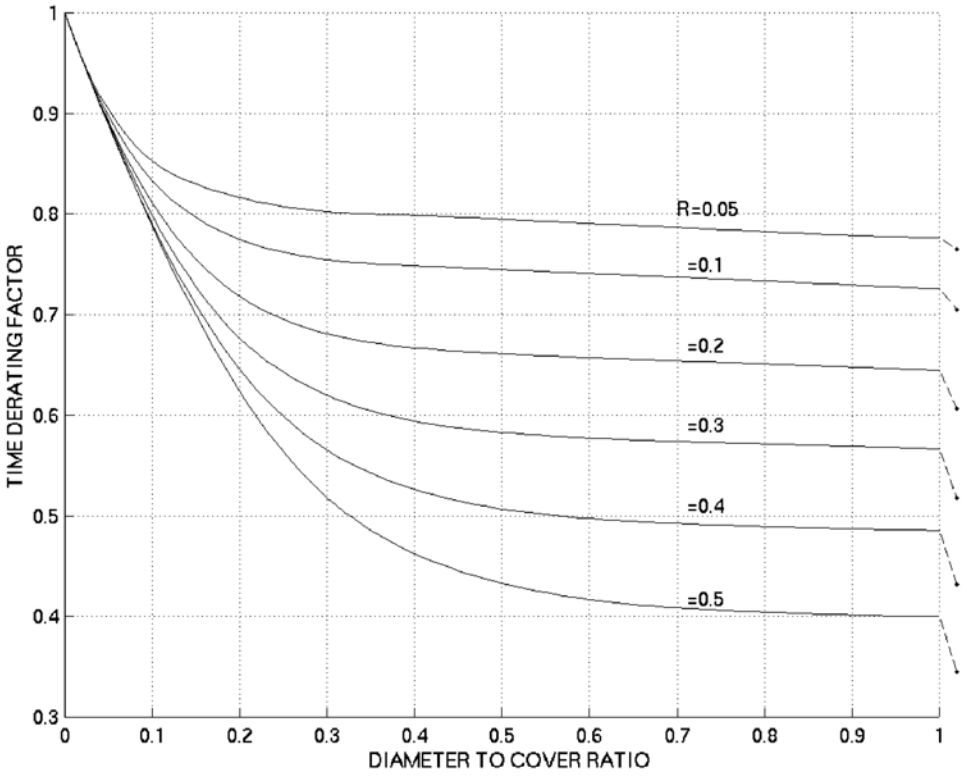

Figure 6.4: Derating factors for two rebar side-by-side splice, planar geometry (Case C) as a function of the rebar to cover ratio Φ/X_c, and $R=C_T/C_S$ the critical concentration ratio. Limiting case for infinite cover ratio shown at right side of graph

Section 7: OTHER COMPLICATING FACTORS

7.1 Cracked specimens

It is noted here that the question of core samples taken from cracked regions has been previously reported [4] although partially covered under the present contract. The principal conclusion of this work was that if significant cracks extend to rebar depth the onset of corrosion will be very rapid. Furthermore core specimens showing abnormally elevated concentrations of total chloride should be suspect and subjecting these specimens to fitting procedures is not likely to produce meaningful results.

7.2 Specimens taken from cylindrical structural elements- fitting core data to a cylindrical model

In some situations cores may have been extracted from structural elements such as cylindrical columns, relatively thin slabs or corner geometries. Under these circumstances a planar, semi-infinite assumption may or may not be justified. The following example represents the analysis of data from a cylindrical column 12" in radius at age 10 years. Synthetic data were generated using a surface concentration C_S of 20, D=4e-9, and C_0=0.2. The following slicing scheme was used.

```
xs=[0 .2 .4 .8 1.2 2.5 4.5]';
 xf=[.19 .39 .79 1.19 1.59 3 5]'
```

Data obtained for the slices is as follows:

```
dclc=[19.1319   17.2991   14.5949   11.2048    8.2298    2.1148  0.2490];
```

and a comparable data set for the equivalent planar case is:

```
dcle =[  19.0562   17.0844   14.2314   10.7348    7.7437    1.8764    0.2574]
```

A small difference is apparent. Attempting to fit the cores to a simple error function results in a nominal 10% error in the diffusion coefficient.

```
Fit to Fickian profile, measured background
 using all data

   Diffusion coefficient = 4.3639e-009
   Surface concentration = 20.0967
.. Background concentration = 0.249
   Residual = 0.023982
```

Fit to Fickian profile, estimated background
using all data
  Diffusion coefficient = 4.4613e-009
  Surface concentration = 20.0754
  Background concentration = 0.12409
  Residual = 0.0077949

Fit to Fickian profile, estimated background
constrained optimization for D,Cs,C0
using all data
  Diffusion coefficient = 4.3609e-009
  Surface concentration = 20.0982
  Background concentration = 0.24841
  Residual = 0.023852

Employing as a model the partial differential equation for diffusion written in cylindrical coordinates results in a much better value for the diffusion coefficient.

Fit cylindrical profile using all data

Fit to cylindrical profile, measured background
  Diffusion coefficient = 3.9207e-009
  Surface concentration = 20.0967
  Background concentration = 0.249
  Residual = 0.015125
  Flag = 1

It should be noted that a 10% variation is not a particularly large discrepancy and it would probably be unnoticed in analysis of real data contaminated with error. It is probably realistic to ignore this difference and treat data from cylindrical columns as a simple planar problem. The method of approach however could be used in other situations of geometrical complexity.

7.3 Analysis of time dependent diffusion coefficients

The possibility that D is a function of time cannot be ignored, although in all cases studied it appears that D decreases in time, making any estimate conservative. For the simple case when D is a function of time only, the solution to the equation is modified, incorporating a new time variable.

As shown in [5] and others, the simple transport equation, for time dependent spatially independent D can be reduced to an equation resembling Fick's second law

$$\frac{\partial C}{\partial T} = L^2 C \qquad 7.1$$

using the transformation

$$T = \int_0^t D(t)dt \qquad 7.2$$

so that for a time independent diffusion coefficient T=Dt. In fact this is what is being measured as pointed out earlier. Since Equation 7.1 also leads to an error function solution, and it is not known beforehand if the diffusion coefficient is time dependent then it must be assumed that what is really being determined in a fitting procedure is a mean value for the diffusion coefficient over the observational time interval. This fact means that future predictions will not be meaningful without some estimate of the functional dependence of D(t) [7].

It was found to be possible to utilize the advanced modeling scheme to fit time dependent diffusion. For purposes of this discussion, a simple exponential model for the diffusion coefficient is assumed

$$D=D_0\exp(-m*t) \qquad 7.3$$

For the same parameters as used in previous discussions, two sets of data were synthesized at age 3 years and 10 years.

At three years the data are

dcl=[17.8642 13.5407 8.1372 3.3843 1.1877 0.2030 0.2000];

Analysis via the advanced fitting method yields:

Fit to Fickian profile, measured background, using all data:

Diffusion coefficient = 2.5921e-009
Surface concentration = 19.9861
Background concentration = 0.2
Residual = 0.00036865

Fit to Fickian profile, estimated background, using all data:

Diffusion coefficient = 2.5894e-009
Surface concentration = 19.9876
Background concentration = 0.20484
Residual = 0.00031134

Fit to Fickian profile, estimated background, constrained optimization for D,Cs,C0 using all data:

Diffusion coefficient = 2.5916e-009
Surface concentration = 19.9848
Background concentration = 0.20074
Residual = 0.00035656

At 10 years

dcl=[18.2889 14.7800 10.0970 5.3372 2.4621 0.2414 0.2000];

Fit to Fickian profile, measured background
using all data
Diffusion coefficient = 1.2148e-009
Surface concentration = 19.9941
Background concentration = 0.2
Residual = 7.3532e-005

Fit to Fickian profile, estimated background
using all data
Diffusion coefficient = 1.2144e-009
Surface concentration = 19.9943
Background concentration = 0.2026
Residual = 5.7638e-005

Fit to Fickian profile, estimated background
constrained optimization for D,Cs,C0
using all data
  Diffusion coefficient = 1.2149e-009
  Surface concentration = 19.9918
  Background concentration = 0.20156
  Residual = 6.6917e-005

The profile of chloride concentration resulting is very similar to an error function but analysis of the slice data will not produce the correct value for the diffusion coefficient. Instead, both sets of data are submitted to analysis, employing the model for D given above.

Fit two time profiles using all data-

Fit to time profile, measured background
  Diffusion coefficient = 4.0137e-009
  time coefficient = 1.0022e-008
  Surface concentration = 19.9861
  Background concentration = 0.2
  Residual = 0.00028486
  Flag = 1

A near perfect fit results. The error in making forward projections using a naïve analysis could be very large. It is noted in passing that efforts to fit the Mangat and Molloy [6] model have not been successful to date. This problem is probably due to difficulties with the function specification and can probably be corrected.

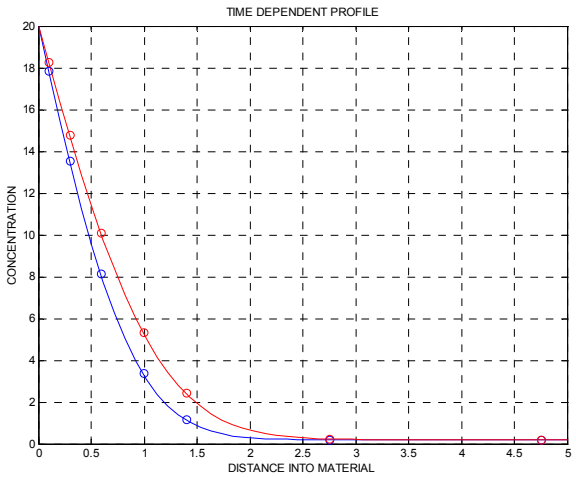

Figure 7.1: Illustrating the resulting time dependent model applied to both data sets

7.4 Alternate boundary conditions

It is worth noting that in addition to a constant environmental concentration, many other conditions may exist at the boundary including various combinations of the following:

> Flux limitation due to film formation in seawater (includes concentration polarization)
>
> Time dependent surface concentration. Sinusoidally varying surface concentration applied to a simple diffusion problem. While a fluctuating surface concentration can produce a "peak" of sorts, the location is near the surface and is itself a function of time. Deeper in the concrete, the profile is virtually identical to the Fickian profile for the average surface concentration. The first slice (which includes the influence of the surface fluctuation) may introduce error into the analysis process. This observation may be another reason for suggesting that the first data point be ignored in actual physical measurements.
>
> Surface layers formed within the concrete with properties differing from the bulk of the concrete possibly due to leaching or plugging of the pores [9].

Using existing programs, it is relatively easy to simulate various simple surface conditions, including flux limitation. Especially if the surface concentration varies at about the same time scale as the characteristic time for diffusion, various peaks and bulges in the chloride profiles may be generated. This portion of the work, while interesting did not seem to produce any significant insights and was discontinued.

It is noted in passing that several other situations could be considered as variations of the cases described above, including flux limited boundary conditions or very thin layers with low permeability (coatings).

7.5 Water transport

In the work reported here, all cases considered involved assuming concrete fully saturated with water. In fact, most of situations of practical interest for corrosion onset occur near the waterline of marine structures or in the splash zone, thus saturation is expected. The consequences of water content at less than 100% are reduced transport (due to partial filling of the pore structure), and the possibility of nondiffusive chloride transport along with water transport Considerable time was invested in a literature review of this latter mechanism. There appears to be little experimental evidence to support several very complicated analytical treatments of this topic [2]. At this time no recommendations are made to include water movement in the proposed transport model developed here. This issue could be reexamined in future work.

A related issue is that of possible leaching of chlorides from structures by fresh water intrusion. Some data gathered from the Sunshine Skyway Bridge suggested altitude

dependence with peaks in the chloride profiles [4]. This topic may warrant further investigation.

7.6 Hard binding models

The advanced modeling technique outlined in Section 4 is not restricted, however and any model could be utilized as a fit for a set of integrated slices. For example consider the limiting case of a hard binding model as a basis for the same fitting procedure used with the error function. Two basis functions are defined for a linear regression in three parameters, C_S, A and C_0 (if C_0 is known it could be inserted as before). A fourth parameter x_f takes the place of the diffusion coefficient. Thus for $x< x_f$,$C=(C_s-A)(1-x/x_f)+A$ and for $x>x_f$,$C =C_0$. This model exhibits a sudden drop of $A-C_0$ at the front. Two basis functions can be defined for optimization.

$$\phi_{0i} = \frac{1}{\delta l_i}\int_{\delta l_i} 1 \cdot dx \qquad 7.4$$

$$\phi_{1i} = \frac{1}{\delta l_i}\int_{\delta l_i} (1-\frac{x}{x_f})dx \qquad 7.5$$

The third parameter x_f, takes the place of the diffusion coefficient as the parameter to be varied during the optimization process, with the slice containing x_f integrated to account for the discontinuity. This formalism is very similar to the previous procedure (utilizing the error function as a basis). The problem is solved for C_S and A. It is also likely that C_0 would be available as a measurement from a deep slice.

Section 8: SENSITIVITY STUDY

Scope

The purpose of this portion of the study was to examine the sensitivity of the elementary analysis method to changes in the manner in which data is presented. To accomplish this task, sets of data were generated by integrating the results of numerical computation, obtained with appropriate modeling assumptions. The following parameters were adopted for all tests: D=4e-9 cm^2/sec, C_T=25 and 2.5 kg/m^3, and a background concentration 0.15 kg/m^3. The threshold concentration for corrosion initiation is 0.71 kg/m^3. Binding is assumed to be present in all cases, (Langmuir isotherm with k=3, C=5 kg/m^3). The coring scheme (slice widths starting from the external surface assuming no wastage) was 0.635, 0.635, 1.27, 1.27, 2.54 and 2.54 cm.

Total chloride profiles were computed (Table 8.1) at 3, 10 and 30 years using the binding model and the binding model with release due to carbonation (stationary front at 0.32 and 0.64 cm), described elsewhere.

Examples

Using synthetic slice data and the Fitter program, evaluate the values of C_S, C_O, D for a variety of test cases. All profiles used in this section were computed using the "soft binding model". Except as noted, all profile fits were made assuming that C_O was known and inserted into the fitting process. These results are summarized in the pages following Table 8.1, which includes the cutting strategies.

Conclusions

Results obtained early (and especially if the first point is omitted) are poor, but generally do not vary by more than a factor of four. As would be expected, some of the worst results are for low concentrations when the interface is deep.

Table 8.1: Schedule of simulated test conditions

				TIME					FRONT	
CASE	Cs=25	Cs=2.5	time=3	time=10	time=30	all slice	skip first	0	0.32	0.64
A	x		x			x		x		
B	x		x				x	x		
C	x		x			x			x	
D	x		x				x		x	
E	x		x			x				x
F	x		x				x			x
G	x			x		x		x		
H	x			x			x	x		
I	x			x		x			x	
J	x			x			x		x	
K	x			x		x				x
L	x			x			x			x
M	x				x	x		x		
N	x				x		x	x		
O	x				x	x			x	
P	x				x		x		x	
Q	x				x	x				x
R	x				x		x			x
AA		x	x			x		x		
BB		x	x				x	x		
CC		x	x			x			x	
DD		x	x				x		x	
EE		x	x			x				x
FF		x	x				x			x
GG		x		x		x		x		
HH		x		x			x	x		
II		x		x		x			x	
JJ		x		x			x		x	
KK		x		x		x				x
LL		x		x			x			x
MM		x			x	x		x		
NN		x			x		x	x		
OO		x			x	x			x	
PP		x			x		x		x	
QQ		x			x	x				x
RR		x			x		x			x

RESULTS

CASE (bs3)		3yr	A	B	
START	END	DATA			
0	0.6	22.0789			
0.7	1.2	8.5072			
1.3	2.5	0.6348			
2.6	3.8	0.1500			
3.9	6.3	0.1500			
6.4	8.9	0.1500			
BACKGROUND CONCENTRATION			0.15	0.15	kg/m3
SURFACE CONCENTRATION			30.62	55.95	kg/m3
RESIDUAL SQUARE ERROR			4.70E-01	1.82E-07	
DIFFUSION COEFFICIENT			3.748E-09	2.191E-09	cm^2/s

CASE (newpl3)		3yr	C	D	
0	0.6	19.6800			
0.7	1.2	8.6480			
1.3	2.5	0.6563			
2.6	3.8	0.1500			
3.9	6.3	0.1500			
6.4	8.9	0.1500			
BACKGROUND CONCENTRATION			0.15	0.15	kg/m3
SURFACE CONCENTRATION			26.65	55.86	kg/m3
RESIDUAL SQUARE ERROR			9.56E-01	1.76E-07	
DIFFUSION COEFFICIENT			4.414E-9	2.223E-9	cm^2/s

0	0.6	17.7490			
0.7	1.2	9.1697			
1.3	2.5	0.8001			
2.6	3.8	0.1500			
3.9	6.3	0.1500			
6.4	8.9	0.1500			
CASE (npl3)		3 yr	E	F	
BACKGROUND CONCENTRATION			0.15	0.15	kg/m3
SURFACE CONCENTRATION			23.45	52.44	kg/m3
RESIDUAL SQUARE ERROR			1.94E+00	2.66E-05	
DIFFUSION COEFFICIENT			5.467E-09	2.458E-09	cm^2/s

CASE (bs10)				G	H	
0	0.6	25.4177				
0.7	1.2	16.7403				
1.3	2.5	7.1262				
2.6	3.8	0.5438				
3.9	6.3	0.1502				
6.4	8.9	0.1500				
BACKGROUND CONCENTRATION				0.15	0.15	kg/m3
SURFACE CONCENTRATION				30.51	32.47	kg/m3
RESIDUAL SQUARE ERROR				9.08E-01	5.76E-01	
DIFFUSION COEFFICIENT				3.697E-9	3.370E-9	cm^2/s

CASE (newpl10)			10 yr	I	J	
0	0.6	22.9533				
0.7	1.2	16.7949				
1.3	2.5	7.1991				
2.6	3.8	0.5586				
3.9	6.3	0.1502				
6.4	8.9	0.1500				
BACKGROUND CONCENTRATION				0.15	0.15	kg/m3
SURFACE CONCENTRATION				27.68	32.47	kg/m3
RESIDUAL SQUARE ERROR				2.93E+00	5.97E-01	
DIFFUSION COEFFICIENT				4.3094E-09	3.399E-9	cm^2/s

CASE (npl10)			10 yr	K	L	
0	0.6	20.7975				
0.7	1.2	16.9232				
1.3	2.5	7.3659				
2.6	3.8	0.6060				
3.9	6.3	0.1503				
6.4	8.9	0.1500				
BACKGROUND CONCENTRATION				0.15	0.15	kg/m3
SURFACE CONCENTRATION				25.36	32.44	kg/m3
RESIDUAL SQUARE ERROR				6.64E+00	6.30E-01	
DIFFUSION COEFFICIENT				5.004E-9	3.475E-9	cm^2/s

CASE (bs30)		30 yr	M	N	
0	0.6	27.2058			
0.7	1.2	21.9398			
1.3	2.5	15.0145			
2.6	3.8	7.4260			
3.9	6.3	1.1967			
6.4	8.9	0.1512			
BACKGROUND CONCENTRATION			0.15	0.15	kg/m3
SURFACE CONCENTRATION			30.28	30.8	kg/m3
RESIDUAL SQUARE ERROR			1.06E+00	9.32E-01	
DIFFUSION COEFFICIENT			3.777E-9	3.6625E-9	cm^2/s

CASE (newpl30)		30 yr	O	P	
0	0.6	24.7037			
0.7	1.2	21.9064			
1.3	2.5	14.9558			
2.6	3.8	7.3568			
3.9	6.3	1.1699			
6.4	8.9	0.1510			
BACKGROUND CONCENTRATION			0.15	0.15	kg/m3
SURFACE CONCENTRATION			28.27	30.8	kg/m3
RESIDUAL SQUARE ERROR			4.05E+00	9.16E-01	
DIFFUSION COEFFICIENT			4.2237E-9	3.631E-9	cm^2/s

CASE (npl30)			Q	R	
0	0.6	22.5122			
0.7	1.2	21.9346			
1.3	2.5	15.0026			
2.6	3.8	7.4146			
3.9	6.3	1.1969			
6.4	8.9	0.1511			
BACKGROUND CONCENTRATION			0.15	0.15	kg/m3
SURFACE CONCENTRATION			26.6	30.8	kg/m3
RESIDUAL SQUARE ERROR			1.03E+01	9.20E-01	
DIFFUSION COEFFICIENT			4.731E-9	3.659E-9	cm^2/s

CASE (bss3)		3 yr	AA	BB	
0	0.6	3.8096			
0.7	1.2	0.7414			
1.3	2.5	0.1571			
2.6	3.8	0.1500			
3.9	6.3	0.1500			
6.4	8.9	0.1500			
BACKGROUND CONCENTRATION			0.15	0.15	kg/m3
SURFACE CONCENTRATION			6.25	12.17	kg/m3
RESIDUAL SQUARE ERROR			1.26E-04	1.67E-07	
DIFFUSION COEFFICIENT			1.620E-9	1.126E-9	cm^2/s

CASE (newp3)		3 yr	CC	DD	
0	0.6	2.4953			
0.7	1.2	0.8804			
1.3	2.5	0.1605			
2.6	3.8	0.1500			
3.9	6.3	0.1500			
6.4	8.9	0.1500			
BACKGROUND CONCENTRATION			0.15	0.15	kg/m3
SURFACE CONCENTRATION			3.56	14.62	kg/m3
RESIDUAL SQUARE ERROR			3.62E-03	3.57E-06	
DIFFUSION COEFFICIENT			2.924E-9	1.1383E-9	cm^2/s

CASE (np3)			EE	FF	
0	0.6	1.7051			
0.7	1.2	1.2674			
1.3	2.5	0.1776			
2.6	3.8	0.1500			
3.9	6.3	0.1500			
6.4	8.9	0.1500			
BACKGROUND CONCENTRATION			0.15	0.15	kg/m3
SURFACE CONCENTRATION			2.2	13.56	kg/m3
RESIDUAL SQUARE ERROR			1.17E-01	2.49E-08	
DIFFUSION COEFFICIENT			7.719E-9	1.484E-9	cm^2/s

CASE (bss10)		10 yr	GG	HH	
0	0.6	4.5963			
0.7	1.2	2.5353			
1.3	2.5	0.5858			
2.6	3.8	0.1543			
3.9	6.3	0.1500			
6.4	8.9	0.1500			
BACKGROUND CONCENTRATION			0.15	0.15	kg/m3
SURFACE CONCENTRATION			5.88	7.65	kg/m3
RESIDUAL SQUARE ERROR			3.94E-02	3.40E-05	
DIFFUSION COEFFICIENT			1.950E-9	1.405E-9	cm^2/s

CASE (newp10)			II	JJ	
0	0.6	3.1066			
0.7	1.2	2.6047			
1.3	2.5	0.6255			
2.6	3.8	0.1552			
3.9	6.3	0.1500			
6.4	8.9	0.1500			
BACKGROUND CONCENTRATION			0.15	0.15	kg/m3
SURFACE CONCENTRATION			3.95	7.6	kg/m3
RESIDUAL SQUARE ERROR			3.90E-01	5.93E-05	
DIFFUSION COEFFICIENT			3.456E-9	1.475E-9	cm^2/s

CASE (np10)		10 yr	KK	LL	
0	0.6	1.9805			
0.7	1.2	2.7882			
1.3	2.5	0.7335			
2.6	3.8	0.1586			
3.9	6.3	0.1500			
6.4	8.9	0.1500			
BACKGROUND CONCENTRATION			0.15	0.15	kg/m3
SURFACE CONCENTRATION			2.83	7.53	kg/m3
RESIDUAL SQUARE ERROR			1.35E+00	1.88E-04	
DIFFUSION COEFFICIENT			6.187E-9	1.662E-9	cm^2/s
CASE (bss30)			MM	NN	
0	0.6	4.9887			
0.7	1.2	3.8204			
1.3	2.5	2.1035			
2.6	3.8	0.5505			
3.9	6.3	0.1658			
6.4	8.9	0.1500			
BACKGROUND CONCENTRATION			0.15	0.15	kg/m3
SURFACE CONCENTRATION			5.82	6.33	kg/m3
RESIDUAL SQUARE ERROR			6.92E-02	2.16E-02	
DIFFUSION COEFFICIENT			1.969E-9	1.719E-9	cm^2/s
CASE (newp30)		30 yr	OO	PP	
0	0.6	3.4395			
0.7	1.2	3.8265			
1.3	2.5	2.1118			
2.6	3.8	0.5563			
3.9	6.3	0.1662			
6.4	8.9	0.1500			
BACKGROUND CONCENTRATION			0.15	0.15	kg/m3
SURFACE CONCENTRATION			4.4	6.33	kg/m3
RESIDUAL SQUARE ERROR			9.90E-01	2.16E-02	
DIFFUSION COEFFICIENT			3.088E-9	1.728E-9	cm^2/s
CASE (np30)		30 yr	QQ	RR	
0	0.6	2.1743			
0.7	1.2	3.8719			
1.3	2.5	2.1823			
2.6	3.8	0.5978			
3.9	6.3	0.1695			
6.4	8.9	0.1500			
BACKGROUND CONCENTRATION			0.15	0.15	kg/m3
SURFACE CONCENTRATION			3.46	6.33	kg/m3
RESIDUAL SQUARE ERROR			2.96E+00	2.35E-02	
DIFFUSION COEFFICIENT			4.706E-9	1.807E-9	cm^2/s

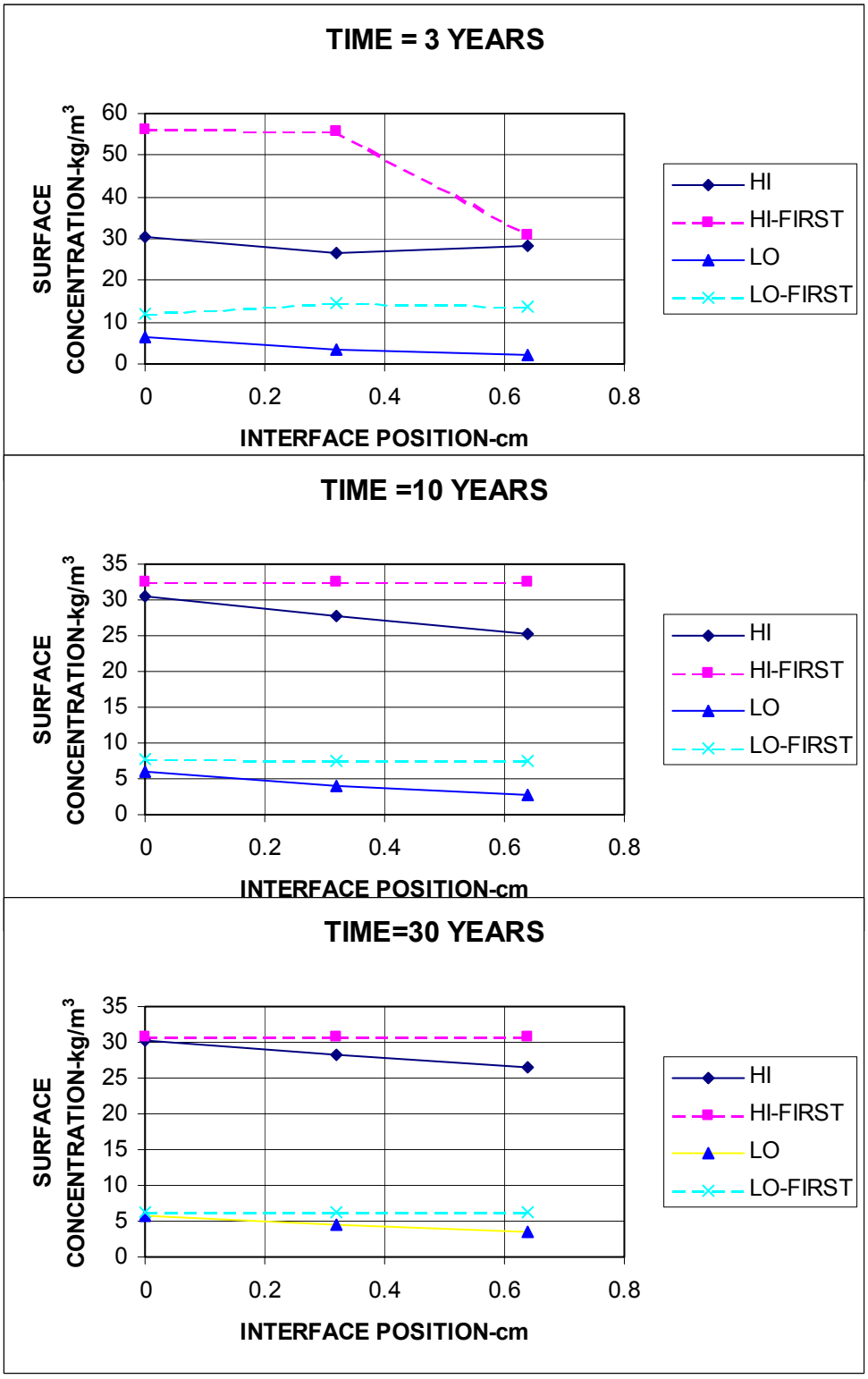

Figure8.1: Effect of interface position on deduced surface concentration with age of specimen.

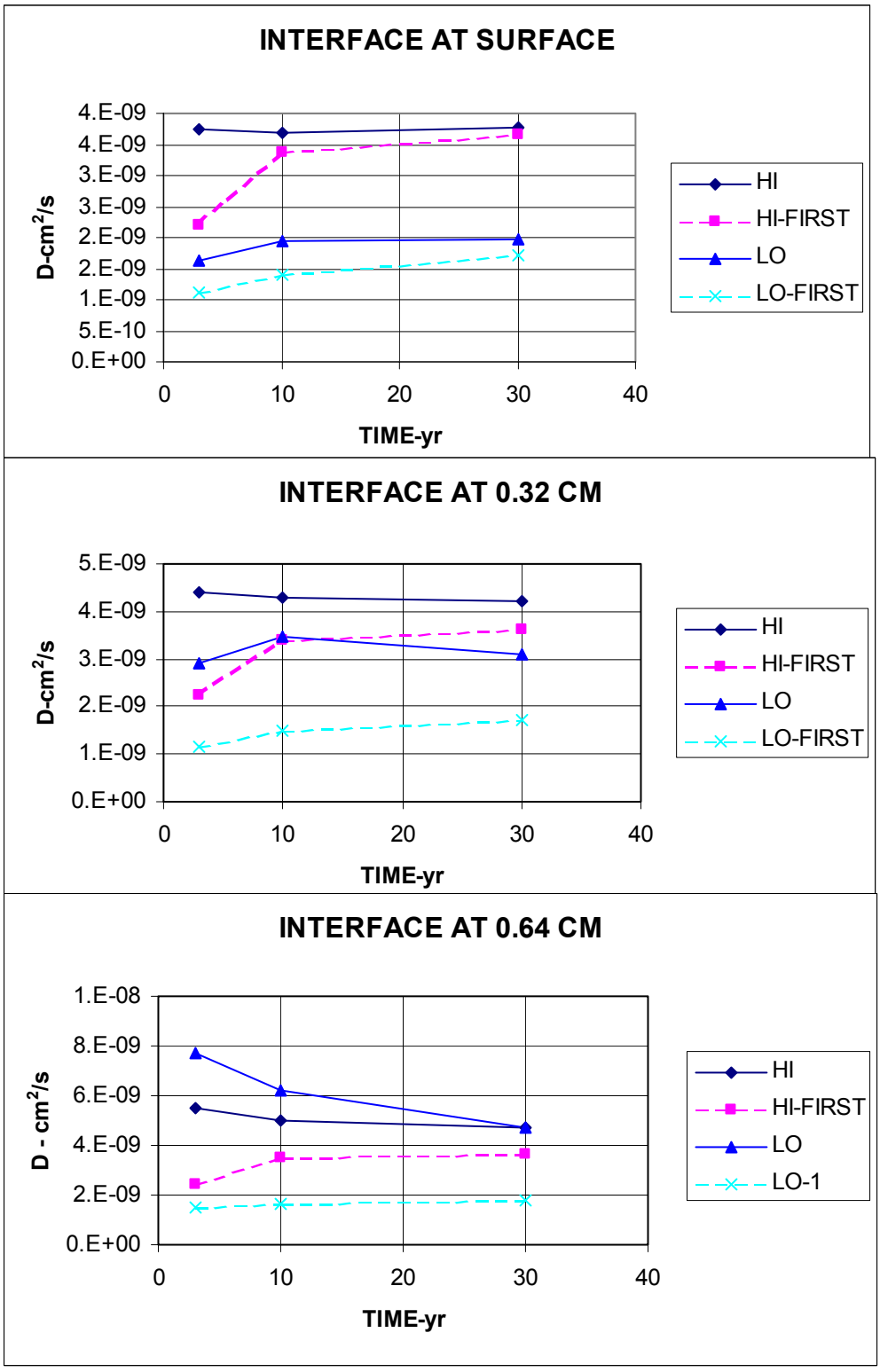

Figure 8.2: Effect of interface position on deduced diffusion rate with age of specimen.

Section 9. REEXAMINATION OF PREVIOUS CORE SAMPLE DATA

Prior to the present study a large collection of core samples from a variety of bridges throughout Florida [25] had been sliced, analyzed and subjected to a fitting procedure to generate C_S, C_0 and D (using an error function model). These data were subjected to the elementary fitting procedure discussed previously (FITTER), including a fit skipping the first slice. In many cases these data were not obtained using a suitable slicing procedure and the results are consequently limited. The results are tabulated in Table 9.1 below. It is significant to note that in most cases the residual error is better than that first obtained, using the previous calculation scheme. After several obvious outliers were removed the data were presented graphically in Figure 9.1.

Table 9.1 Reexamination of previous data.

IDENT	AGE (YR)	THIS STUDY					PREVIOUS RESULTS		
		D IN^2/YR	CS KG/M^3	C0 KG/M^3	ERROR	R^2	D IN^2/YR	CS KG/M^3	C0 KG/M^3
PC2	12	0.0187	29.39	0.142	9.9E-06	1.0E+00	0.018	30	0.15
GRN	6	0.0166	13.88	0.125	4.5E-04	1.0E+00	0.019	17	0.1
GRN	6	0.0189	18.91	0.095	5.0E-05	1.0E+00	0.017	20	0.1
GRN	6	0.0402	1.23	0.075	4.7E-05	1.0E+00	0.043	1.2	0.08
GRN	6	0.0465	16.88	0.29	7.3E-02	1.0E+00	0.047	17	0.17
7MI	9	0.02	26.55	13.798	9.3E-08	1.0E+00	1.25	20	2.5
7MI	9	0.2745	19.28	5.716	3.3E-01	1.0E+00	0.28	19.3	2.5
7MI	6	0.1907	17.99	5.054	9.2E-04	1.0E+00	0.98	16.5	2.5
7MI	6	2.8365	17.6	0	2.7E+00	9.5E-01	1.87	18	2.5
7MI	6	1.9052	19.43	0	4.1E+00	9.6E-01	1.52	19	2.5
7MI	6	0.974	13.65	0	1.3E-01	1.0E+00	0.54	14	2.5
7MI	6	1.3566	6.1	0	1.9E-01	9.8E-01	0.32	6.3	2.5
7MI	6	5.5029	3.63	0.066	1.4E+00	5.4E-01			
7MI	6	0.0038	1.11	2.703	8.8E-01	2.4E-01			
75N	11	0.0416	18.9	0.101	3.3E-02	1.0E+00	0.045	18	0.16
75N	11	0.0278	11.59	0.159	1.4E-02	1.0E+00	0.028	11.5	0.17
75S	11	0.0101	16.72	0.139	9.5E-03	1.0E+00	0.011	16	0.11
75S	11	0.0155	25.39	0.169	2.5E-03	1.0E+00	0.016	25	0.15
HAL	5	0.2826	12.02	0	1.7E+00	9.9E-01	0.31	11	0.2
IR1	6	0.2474	14.84	0.16	2.6E-01	1.0E+00	0.27	14	0.16
IR2	6	1.1991	12.9	0	4.8E+00	9.5E-01	1.18	13	0.2
NWR	10	0.0699	1.17	0.13	2.1E-03	1.0E+00	0.069	1.2	0.12
ITA	3	0.1811	3.3	0.125	1.4E-03	1.0E+00	0.17	3.5	0.1
ITA	3	0.0548	1.21	0.088	4.7E-03	9.9E-01	0.082	1	0.1
ITB	3	0.0079	16.94	0.032	4.8E-04	1.0E+00	0.023	10	0.03
ITB	3	0.0012	14.27	0.018	2.8E-04	1.0E+00	0.027	3	0.01
VA1	9	1.5502	14.75	0	9.1E+00	9.0E-01	1.42	15	0.4
VA1	9	0.7232	3.06	2.053	1.7E-01	8.7E-01	1	3	2
VA2	9	0.3232	30.33	5.364	5.8E+00	9.9E-01	0.76	28	0.4
VA2	9	0.6029	21.02	2.774	2.6E+00	9.9E-01	0.98	20	0.4

AL1	10	0.0097	2.69	0.28	1.8E-03	1.0E+00	0.008	3	0.27
AL1	10	0.161	1.7	0.258	3.6E-02	9.8E-01	0.15	1.7	0.29
AL2	10	0.1211	12.51	0.347	8.2E-03	1.0E+00	0.12	12.5	0.3
AL2	10	0.1222	1.35	0.23	2.5E-02	9.7E-01	0.1	1.4	0.27
SNK	11	0.5909	4.88	1.498	1.3E+00	9.1E-01	0.41	5	1.8
SNK	11	0.6103	6.16	1.329	2.0E+00	9.3E-01	0.39	6.5	1.8
MAT	12	0.0185	75.36	0.131	1.7E-03	1.0E+00	0.018	76	0.16
MAT	12	0.0166	37.07	0.144	7.8E-03	1.0E+00	0.019	35	0.11
MAT	12	0.0541	0.95	0.012	7.0E-05	1.0E+00	0.061	0.9	0.01
PC1	9	0.0539	47.31	0.183	7.3E-02	1.0E+00	0.059	45	0.2
PC1	9	0.0394	23.54	0.161	9.3E-03	1.0E+00	0.041	23	0.13
PC1	9	0.0427	1.86	0.109	8.5E-03	9.9E-01	0.037	2	0.1
PC2	12	0.0289	30.72	0.107	1.5E-03	1.0E+00	0.031	30	0.08
PC2	12	0.0125	25.37	0.174	6.0E-03	1.0E+00	0.013	25	0.16
PC2	12	0.0187	29.39	0.142	9.9E-06	1.0E+00	0.018	30	0.15
PC2	12	0	79.26	0.29	9.1E-02	9.0E-01	0.01	2	0.3
PC3	12	0.0165	37.67	0.2	5.0E-03	1.0E+00	0.017	37	0.14
PC3	12	0.0156	21.89	0.177	7.9E-03	1.0E+00	0.019	20	0.13
CHO	13	1.5691	9.29	0	8.6E-02	9.9E-01	1.38	9.4	0.3
CHO	13	0.0412	6.47	0.237	3.1E-02	1.0E+00	0.043	6.4	0.2
PER	11	0.014	45.59	0.21	9.0E-03	1.0E+00	0.015	45	0.2
PER	11	0.0077	9.31	0.288	3.8E-02	1.0E+00	0.01	8.2	0.3
PER	11	0.0077	21.75	0.405	3.4E-03	1.0E+00	0.009	20	0.36
APA	4	0.1356	0.61	0.39	7.5E-03	8.3E-01	4.53	0.5	0.3
APA	4	1.5053	0.52	0.362	5.0E-03	8.3E-01	0.96	0.5	0.39
APA	4	0.0571	4.61	0.367	8.7E-04	1.0E+00	0.062	4.5	0.34
APA	4	0.0146	0.48	0.37	1.0E-03	6.6E-01	20.7	0.5	0.15
IT2	9	0.0669	3.38	0.224	6.1E-03	1.0E+00	0.064	3.5	0.2
IT2	9	0.8729	2.69	0	3.0E-01	9.3E-01	0.64	2.7	0.3
IT2	9	0.0233	1.76	0.197	2.1E-02	9.8E-01	0.049	1.4	0.15
IT3	9	0	61.32	0.27	2.0E-04	1.0E+00	0.009	2.4	0.26
IT3	9	0.4041	10.17	0.504	2.6E-01	1.0E+00	0.45	10	0.3
IT3	9	0.0464	1.39	0.109	6.2E-07	1.0E+00	0.045	1.4	0.11
NWP	6	0.1105	49.43	1.202	3.1E+00	1.0E+00	0.12	49	0.3
NWP	6	0.0187	0	0.439	1.0E+00	1.5E-01	0.3	0.7	0.3
NWP	6	0.0171	48.92	0.188	9.7E-03	1.0E+00	0.014	54	0.27
NWP	6	0.0489	4.52	-0.045	1.1E-07	1.0E+00	0.002	20	0.26
HOB	6	0.2128	1.4	0.334	1.1E-03	1.0E+00	0.2	1.4	0.35
HOB	6	0.0826	0.97	0.409	7.6E-03	9.7E-01	0.077	1	0.41
HOB	6	0.8436	6.2	0	4.1E+00	9.2E-01	0.75	6	0.4
HOB	6	0.035	1.45	0.405	5.5E-05	1.0E+00	0.039	1.4	0.4
IT4	11	0.0381	0.73	0.2	4.3E-02	8.2E-01	0.65	0.5	0.15
IT4	11	0.3977	0.92	0.046	4.4E-01	7.1E-01	0.34	0.9	0.1
IT4	11	0.3542	12.18	0	5.4E-01	1.0E+00	0.35	12	0.22
IT4	11	0.4848	0.96	0	1.0E-01	6.8E-01	0.9	0.7	0.3
MI1	8	0	49.88	0.153	5.3E-04	1.0E+00	0.018	1	0.15
MI1	8	0.037	1.34	0.158	3.3E-04	1.0E+00	0.028	1.5	0.15
MI1	8	0.0077	1.06	0.157	6.5E-05	1.0E+00	0.012	0.9	0.15
MI2	8	0.0194	3.66	0.16	2.1E-04	1.0E+00	0.022	3.5	0.15
MI2	8	0.0194	1.85	0.171	5.3E-06	1.0E+00	0.022	1.8	0.15
MI2	8	0.1349	3	0.128	4.4E-03	1.0E+00	0.12	3.2	0.15
MI2	8	0.1069	3.44	0.141	1.4E-02	1.0E+00	0.1	3.5	0.15

SSK	7	0.0212	20.25	0.235	3.3E-03	1.0E+00	0.022	20	0.2
SSK	7	0.0428	3.73	0.207	4.8E-04	1.0E+00	0.041	3.8	0.2
SSK	7	0.0204	19.22	0.364	3.8E-01	1.0E+00	0.026	17.5	0.2
SSK	7	0.0177	46.15	0.271	2.1E-04	1.0E+00	0.019	45	0.25
SSK	7	0.0168	37.72	0.247	4.6E-04	1.0E+00	0.015	40	0.23
SSK	7	0.018	35.49	0.302	8.7E-04	1.0E+00	0.018	36	0.3
SSK	7	0.0163	40.24	0.348	5.7E-03	1.0E+00	0.016	41	0.35
SSK	7	0.0218	41.84	0.354	5.0E-04	1.0E+00	0.022	41.8	0.35
SSK	7	0.0173	41.76	0.169	7.9E-07	1.0E+00	0.019	40	0.2
SSK	7	0.0077	73.73	0.327	4.4E-03	1.0E+00	0.012	60	0.25
SSK	7	0.0077	52.56	0.273	4.8E-05	1.0E+00	0.009	50	0.25
SSK	7	0.0012	55.4	0.187	6.7E-05	1.0E+00	0.004	30	0.25
SSK	7	0.0077	128.36	0.541	1.0E-02	1.0E+00	0.015	95	0.25
SSK	7	0.0077	69.83	0.226	2.2E-03	1.0E+00	0.011	60	0.25
SSK	7	0.0278	34.38	0.315	1.5E-02	1.0E+00	0.027	35	0.25
SSK	7	0.0077	49.65	0.223	2.0E-03	1.0E+00	0.012	40	0.25
SSK	7	0.0175	31.77	0.18	2.0E-04	1.0E+00	0.017	32	0.18
NIL	5	4.358	11.01	0	2.4E+00	7.6E-01	6.08	10	0.3
NIL	5	0.0783	32.67	8.452	1.1E+00	1.0E+00	0.46	25	0.3
NIL	5	0.532	13.65	0.204	4.5E-01	1.0E+00	0.33	13.5	0.3
NIL	5	0.1435	9.79	2.835	2.7E-07	1.0E+00	0.34	9	0.3
NIL	5	0.295	6.71	0	2.2E-02	1.0E+00	0.14	7.15	0.3
NIL	5	0.1483	4.38	0.018	9.7E-03	1.0E+00	0.089	4.5	0.01
NIL	5	0.9202	23.7	3.325	3.8E+00	9.9E-01	0.76	25	0.3
NIL	5	0.4124	28.75	0	0.14059	0.99979	0.23	30	0.3
NIL	5	0.588	7.92	0	1.19671	0.98135	0.33	8	0.3

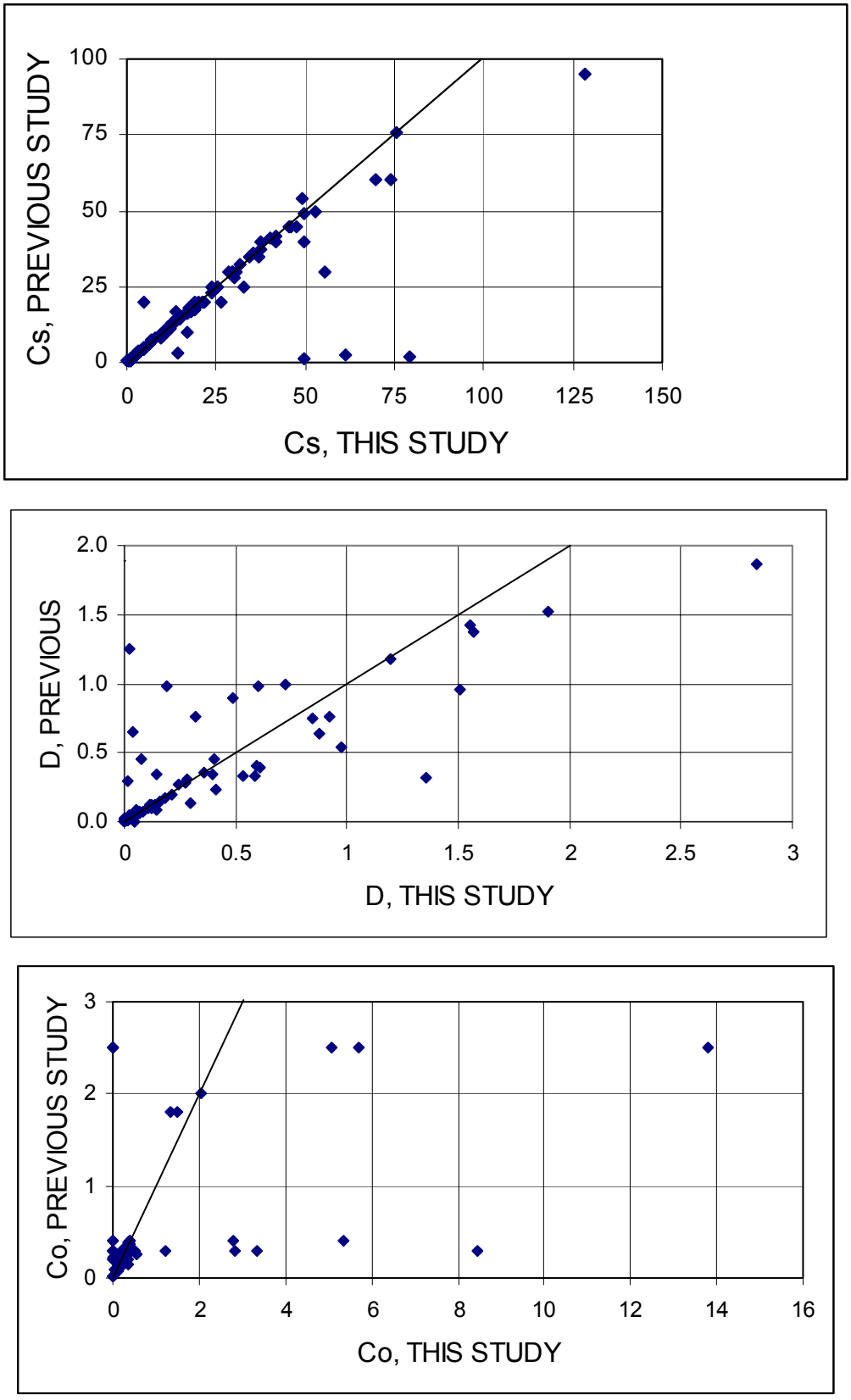

Figure 9.1. Comparison of diffusion parameters obtained with the previous procedure and in this study using the FITTER program. See Table 9.1 for units used.

Section 10. PRINCIPAL CONCLUSIONS

The conduct of the research reported here has:

1. Produced several numerically sound approaches to determining the (Fickian) parameters C_S, C_0 and D for sliced specimens, requiring no operator intervention. Methods can handle arbitrary slice dimensions including cut wastage. It was pointed out that both estimation of C_0 and assumption of last slice data to obtain the background are valuable techniques. Sources of error have been distinguished and discussed as follows. a) The error associated with model fitting to experimental data, assuming the experimental data is accurate. b) The influence of error in analysis (either relative or absolute) has on the determination of model parameters. c) The improvement in fit to model that may result from the choice of slicing dimensions.

2. Investigated the results from several computational models to determine the variation in the profile for different assumptions. Developed several alternative approaches to fitting slice data, capitalizing on the observation that many profiles still maintain a “square root of time” dependence even if not Fickian. These techniques permit forward prediction of chloride intrusion. Coupled with a binding isotherm this method may be much more successful at estimating the time to initiation of corrosion than the use of a Fickian model.

3. Examined the effect of surface layers (produced by carbonation, etc) which evidently produce “peaks” in the profile data. One principal conclusion from this portion of the present effort is that relatively simple modeling provides a satisfactory estimate of the chloride profile and that furthermore the carbonation/release mechanism has little or no effect on the total chloride profile ahead of the carbonation front. Thus a square root of time dependence is maintained. This effort also extended items 1 and 2 above to handle this problem. To some extent the influence of this mechanism on predictions of chloride intrusion can be mitigated by treating the first slice separately, but the loss of one data point has a significant effect on accuracy.

4. Developed a slicing strategy intended to optimize the prediction of chloride intrusion and minimize costs associated with analysis. If implemented, this strategy may minimize wasted analysis steps. It is recommended that a deep slice be utilized to provide an estimate of background concentration rather than attempting to fit this parameter.

5. Reevaluated and extended analysis of current database. As one part of this portion of the effort, the effect of cracks in the concrete cover was further examined. If the background slice concentration is abnormally high or above the critical level then the core is possibly from a cracked concrete location and no substantial information can be gained from fitted parameters.

6. Investigated extension of damage function modeling based on information gathered to date. Part of this effort included an extension of modeling to predict derating of cover due to the diffusional blocking effect of the rebar itself.

7. Developed a new fitting procedure to include binding. If the potential for physico-chemical binding exists, the choice of a model for chloride intrusion will be impacted. Efforts were made to predict the influence on the determination of Fickian parameters. It is concluded that binding will produce conservative results, but not result in accurate predictions of time to initiation. An advanced binding model was developed and tested. This model produces an isotherm from total chloride data alone.

8. Prepared for delivery a spreadsheet program to accomplish the fitting procedure outlined in item 1 above. Other programs developed during the conduct of this research are open and available but are not intended for delivery.

9. Analyzed fitting procedures including time dependent diffusion and cylindrical geometries using procedures developed under item 7 above. It is tentatively concluded that cores cut from typical cylindrical piles can be analyzed by assuming planar geometry.

BIBLIOGRAPHY

[1] A. Sagüés, S. Kranc and F. Presuel-Moreno, “Applied Modeling for Corrosion Protection Design for Marine Bridge Substructures”, Report No. 0510718, June, 1997, available from Florida Department of Transportation, Research Center, Tallahassee, Florida.

[2] Saetta, A., Scotta, R. and Vitaliani, R., "Analysis of Chloride Diffusion into Partially Saturated Concrete", ACI Materials Journal, Vol 47, pp.441-451, 1993

[3] Xi, Y., and Bazant, Z., “Modeling Chloride Penetration In Saturated Concrete”, J. Materials in Civil Engineering, Vol. 11, p. 58-65, 1999.

[4]Sagüés, A.A., Kranc, S.C., Presuel-Moreno, F; Rey, D., Torres-Acosta, A. and Yao, L., “Corrosion Forecasting for 75-Year Durability Design of Reinforced Concrete”, Final Report to Florida Department of Transportation, Report No. BA502, December 31, 2001. Available through National Technical Information Service, Springfield, VA, or Florida Department of Transportation Research Office, Tallahassee, Fl.

[5]Crank, J., The mathematics of Diffusion, 2nd Edition (Oxford, UK: Oxford University Press, 1975)

[6] P.S. Mangat, J.M. Khatib, B.T. Molloy, Cement & Concrete Composites 16 (1994): p. 73.

[7] Bamforth, P. B., “The Derivation Of Input Data For Modelling Chloride Ingress From Eight-Year UK Coastal Exposure Trials”, Magazine of Concrete Research, Vol. 51, p.87-96, 1999

[8] N.S. Berke, M.C. Hicks, “Estimating The Life Cycle Of Reinforced Concrete Decks And Marine Piles Using Laboratory Diffusion And Corrosion Data,” pp. 207-231 in Corrosion Forms and Control for Infrastructure, ASTM STP 1137, Victor Chaker, Ed., American Society for Testing and Materials, Philadelphia, 1992.

[9] Andrade, C., Diez, J.M., and Cruz Alonso, M., “Mathematical Modeling Of A Concrete Surface “Skin Effect” On Diffusion In Chloride Contaminated Media”, Advn. Cem. Bas. Mat., Vol.6, p.39-44, 1997.

[10]Nilsson, L. Construction and Building Materials, Vol. 10, p.301 (1996)

[11]Sagüés, A.A., “Modeling the Effects of Corrosion on the Lifetime of Extended Reinforced Concrete Structures” , Topical Research Symposium, Corrosion/2003, NACE International, Houston, 2003.

[12] Tang, L., Cement and Concrete Research, Vol. 29, p. 1463 (1999)

[13] Nilsson, L.O., Massat, M., and Tang, L., "The Effect of Non-linear Chloride Binding on the Prediction of Chloride Penetration into Concrete Structures", p. 469 in Durability of Concrete, ACI Publication SP-145, V.M. Malhotra, Ed., American Concrete Institute, Detroit, 1994.

[14]Atkinson, A. and Nickerson, A.K., Journal of Materials Science, Vol. 19, p.3068, 1984.

[15]Baer, J., Dynamics of Fluids in Porous Media, Dover Publications, Inc., New York, 1988.

[16]Sandberg, P., Cement and Concrete Research, Vol.29, p.473 (1999)

[17] J. Tritthart, "Chloride Binding in Cement, II", Cement and Concrete Research, Vol. 19, pp. 683-691, 1989.

[18] Rasheeduzzafar, S. Hussain and S. Al-Saadoun, "Effect of Cement Composition on Chloride Binding and Corrosion of Reinforcing Steel in Concrete", Cement and Concrete Research, Vol.21, pp. 777-794, 1991.

[19] Tang, L. and Nilsson, L.O., “Chloride Binding Capacity And Binding Isotherms Of OPC Pastes And Mortars”, Cement and Concrete Research, Vol. 23, p. 247-253, 1993.

[20] “In-Core Leaching of Chloride for Prediction of Corrosion of Steel in Concrete”, A.A. Sagüés, S.C. Kranc, L. Caseres, L.Li and R.E. Weyers, p. 109 in Long Term Durability of Structural Materials, P.J.M. Monteiro, K.P. Chong, J. Oarsen-Basse and K. Komvopoulus, Eds., Elsevier Science Ltd., Amsterdam, 2001.

[21] K. Tuutti, "Corrosion of Steel in Concrete" (ISSN 0346-6906), Swedish Cement and Concrete Research Institute, Stockholm, 1982.

[22] A. Sagüés, E. Moreno, W. Morris and C. Andrade, "Carbonation in Concrete and Effect on Steel Corrosion", Final Report No. WPI 0510685 to Florida Department of Transportation , available from Florida DOT Research Center, Tallahassee, Fla., 1997.

[23] "Decreased Corrosion Initiation Time of Steel in Concrete due to Reinforcing Bar Obstruction of Diffusional Flow", S.C Kranc, A.A. Sagüés and Presuel-Moreno, F.J., ACI Materials Journal, Vol. 99, p.51, 2002

[24] Sagüés, A.A. and Kranc, S.C. "Effect of Structural Shape and Chloride Binding on Time to Corrosion of Steel in Concrete in Marine Service", , p. 105-114 in Corrosion of Reinforcement in Concrete Construction, C.L. Page, P.B. Bamforth and J.W. Figg, Eds, The Royal Society of Chemistry, Cambridge, 1996.

[25] A.A. Sagüés, "Corrosion of Epoxy-Coated Rebar in Florida Bridges", Final Report to Florida D.O.T., WPI No. 0510603, May, 1994, available from Florida Department of Transportation, Research Center, Tallahassee, Florida.

UNIT CONVERSIONS TABLE

CONVERSION FACTORS, US CUSTOMARY TO METRIC UNITS

Multiply	***by***	***to obtain***
inch	25.4	mm
foot	0.3048	meter
square inches	645	square mm
cubic yard	0.765	cubic meter
pound/cubic yard	0.593	kg/cubic meter
$inch^2$/year	$2.046\ 10^{-7}$	cm^2/sec
gallon/cubic yard	4.95	liter/cubic meter
standard cubic feet/hour	466.67	ml/minute
ounces	28.35	gram
pound	0.454	kilogram
pound (lb)	4.448	newtons
kip (1000 lb)	4.448	kilo newton (kN)
pound/in^2	0.0069	MPa
kip/in^2	6.895	MPa
ft-kip	1.356	kN-m
in-kip	0.113	kN-m